Experimental Basis — 1

Lecture 1

- An example analysis
- How to design a good experiment
- Experiments

Lecture 2

- Triggers
- Techniques
- Soft skills
- The future

26/05/2023 — FPCP pre-conference school
[indico]

Patrick Koppenburg
[@pkoppenburg@sciencemastodon.com] [@pkoppenburg] [patrick.koppenburg@nikhef.nl]
Nikhef


25/05/2023 - patrick@koppenburg.ch

BLUF — Bottom Line Up Front

- Analyses exploit strengths of experiments
- Experiment designs are driven by physics
- There are multiple choices which leads to complementary experiments

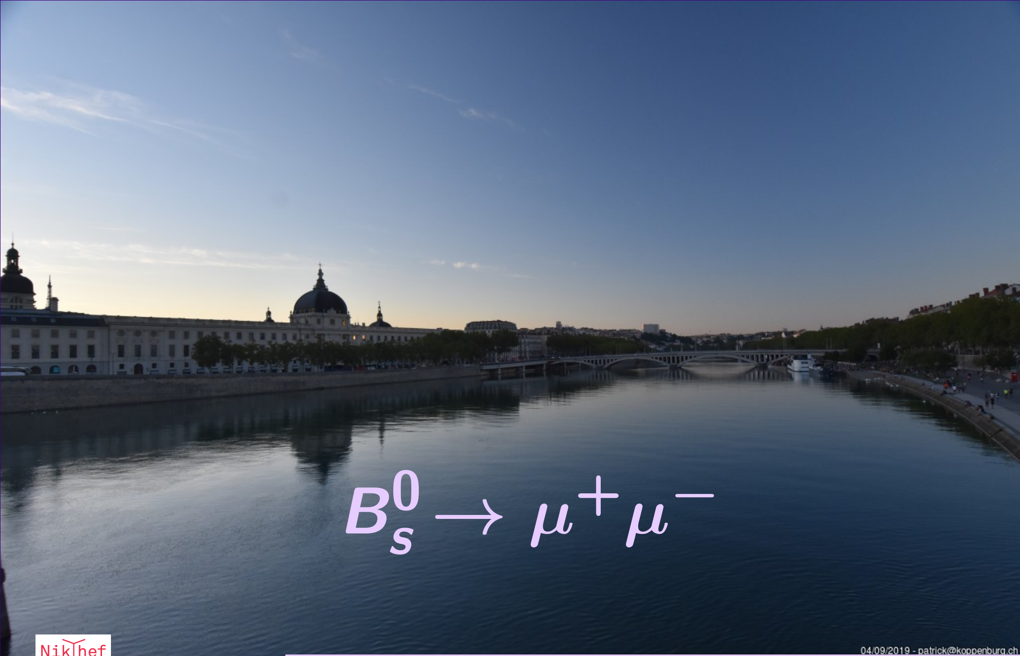

$B_s^0 \to \mu^+\mu^-$

$B_s^0 \to \mu^+\mu^-$

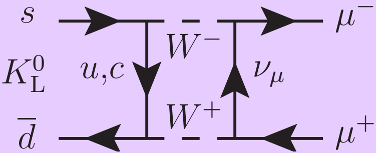

- Start with $K_L^0 \to \mu^+\mu^-$

$B_s^0 \to \mu^+\mu^-$

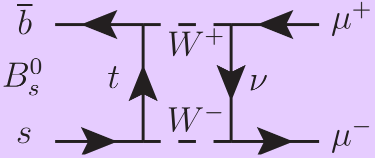

- Replace quarks by b and $\overline{s}$ (for B_s^0) and t ($\propto V_{tb}V_{ts}$)

$B_s^0 \to \mu^+\mu^-$

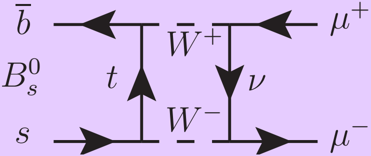

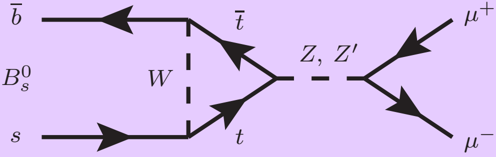

- Replace quarks by b and $\bar{s}$ (for B_s^0) and t ($\propto V_{tb}V_{ts}$)
- Add a penguin contribution ($\propto V_{tb}V_{ts}$)

$B_s^0 \to \mu^+\mu^-$

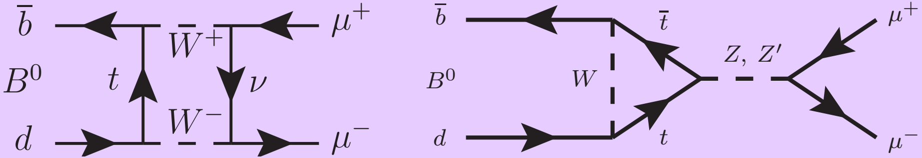

- Replace quarks by b and $\bar{s}$ (for B_s^0) and t ($\propto V_{tb}V_{ts}$)
- Add a penguin contribution ($\propto V_{tb}V_{ts}$)
- For $B^0 \to \mu^+\mu^-$ suppress by $V_{tb}V_{td}$ instead

$B_s^0 \to \mu^+\mu^-$ PREDICTION

Very rare decay, well described in the SM

$$\mathcal{B}(B_s^0 \to \mu^+\mu^-)_{\rm SM} = (3.66 \pm 0.14) \cdot 10^{-9}$$

[Beneke, Bobeth, Szafron, JHEP 10 (2019) 232, arXiv:1908.07011],
[Bobeth, Gorbahn, Hermann, Misiak, Stamou, Steinhauser, PRL 112, 101801 (2014)],
[De Bruyn, Fleischer, Knegjens, PK, Merk, Pellegrino, Tuning, PRL 109, 041801 (2012)] ...

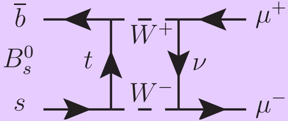

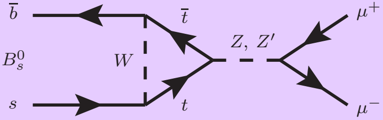

Very sensitive to NP, e.g. Minimal supersymmetric Models:

$$\mathcal{B}(B_s^0 \to \mu^+\mu^-)_{\rm MSSM} \propto \frac{m_b^2 m_\ell^2 \tan^6\beta}{m_A^4}$$

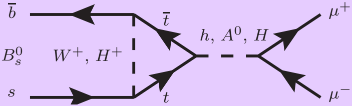

$B_s^0 \to \mu^+\mu^-$ Limits History

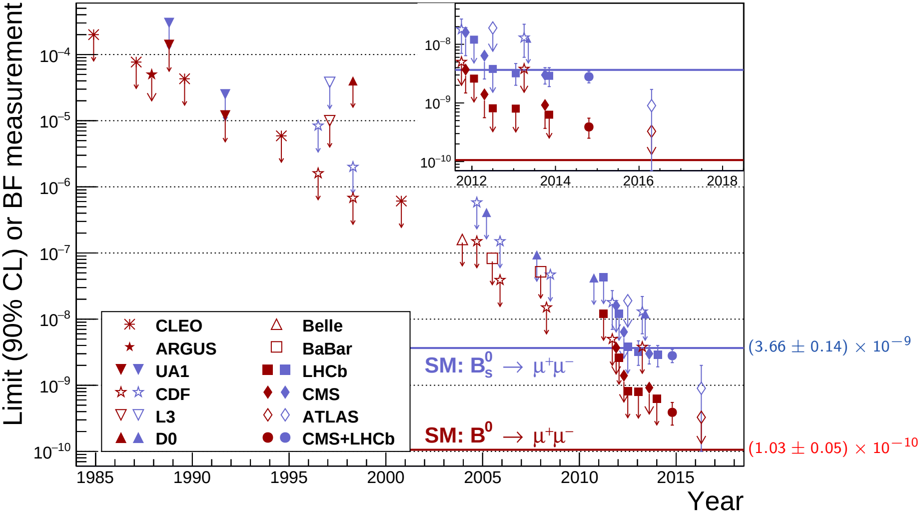

How is $B_s^0 \to \mu^+\mu^-$ measured?

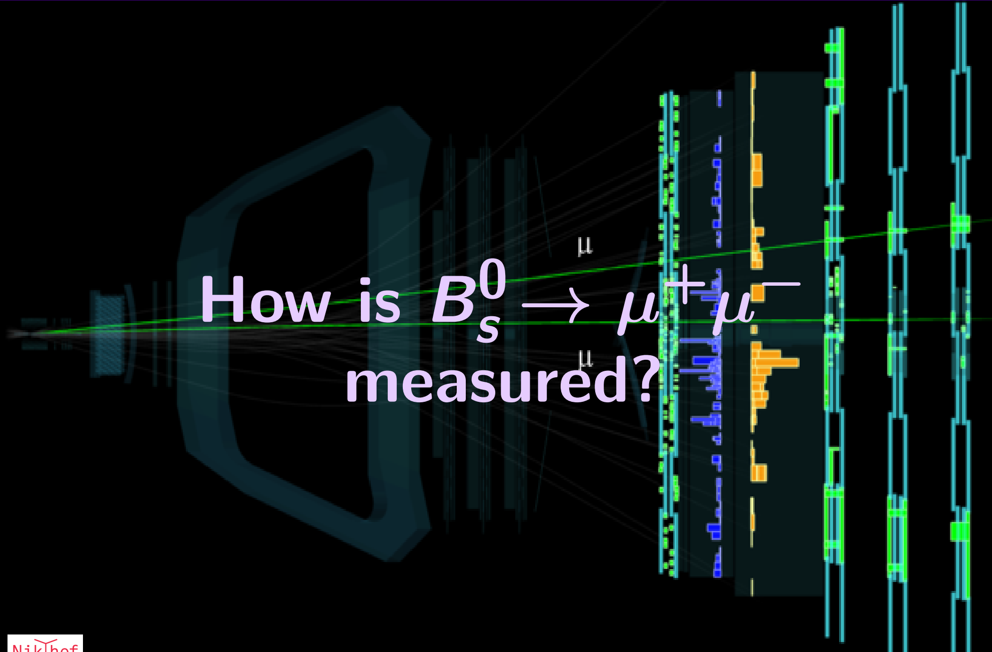

LHCb

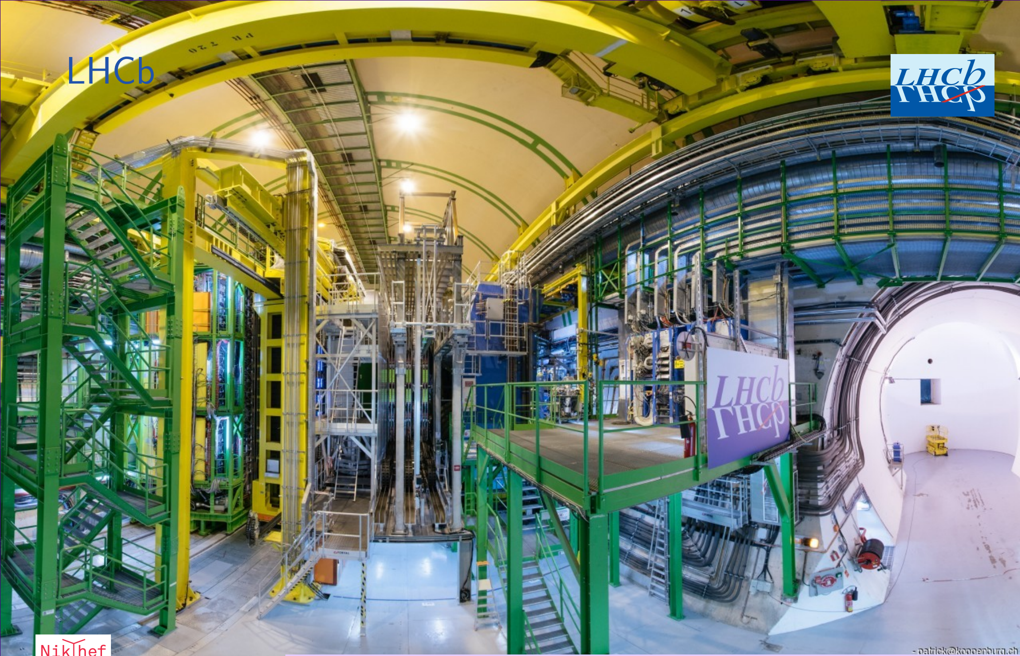

LHCb

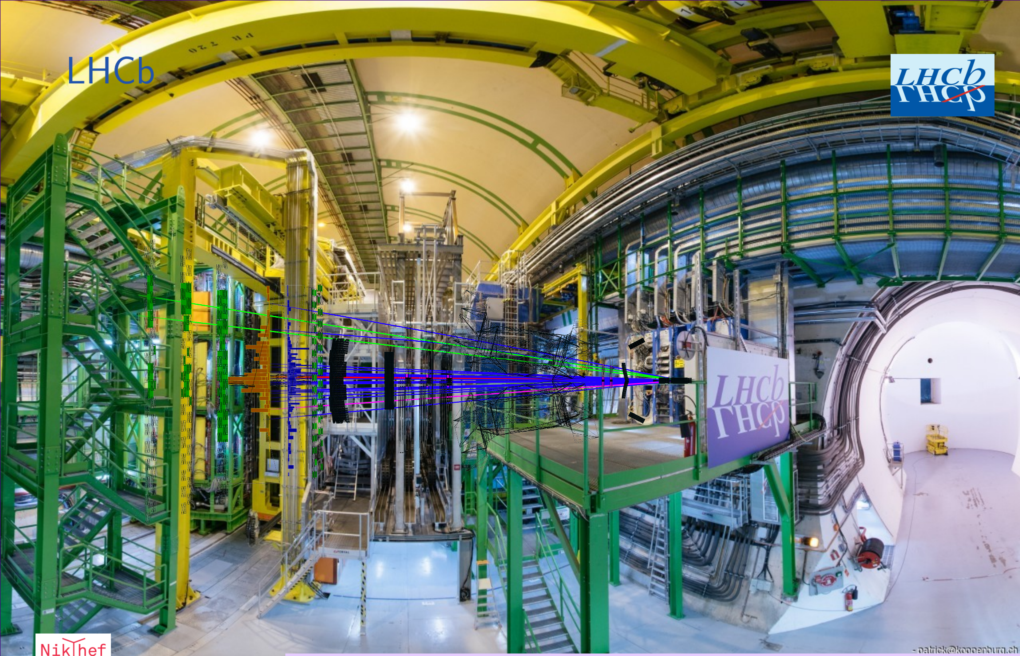

Dimuon mass distribution

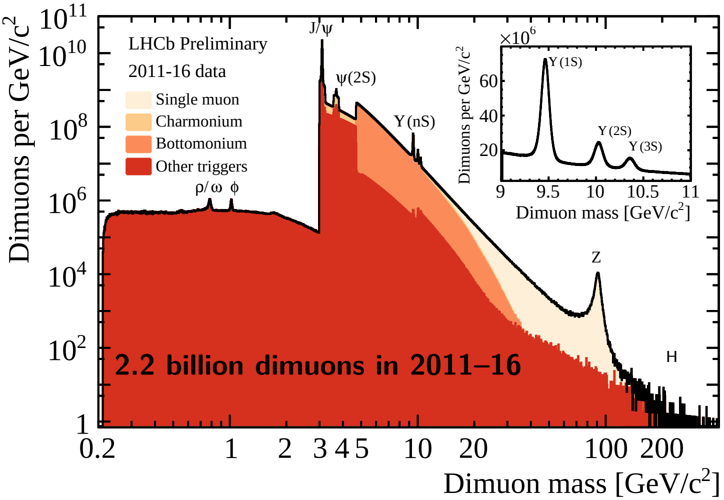

Dimuon mass distribution

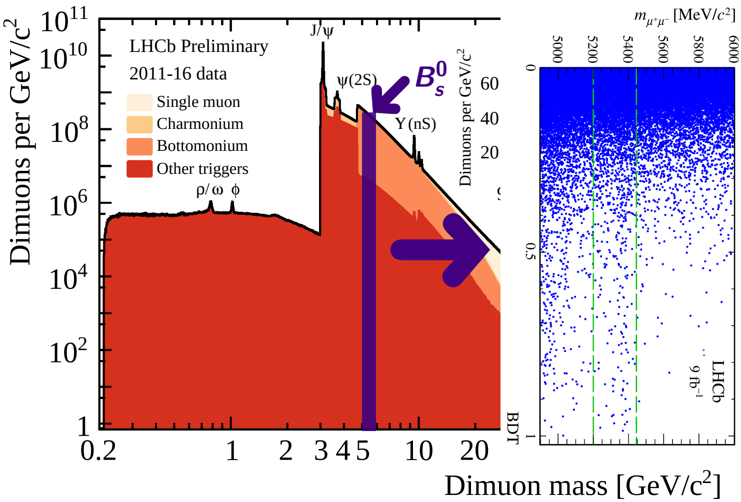

Legacy measurement of $B_s^0 \to \mu^+\mu^-$

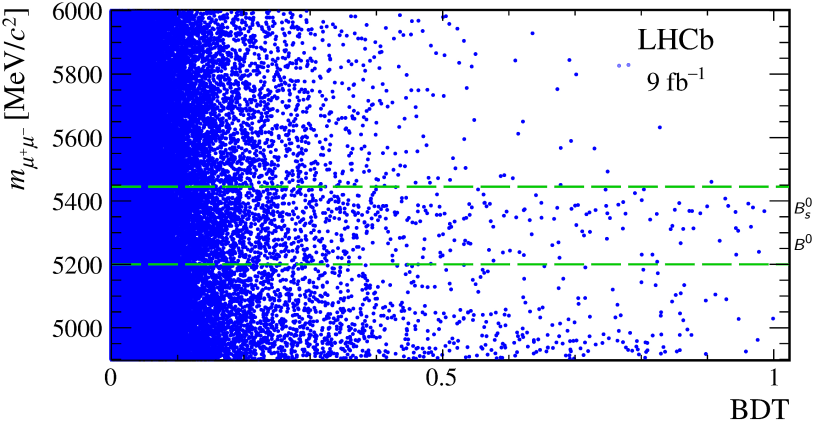

$B \to \mu^+\mu^-$ search using 2011–2018 data (9 fb^{-1}) is done with a mass fit in bins of BDT output.

LEGACY MEASUREMENT OF $B_s^0 \to \mu^+\mu^-$

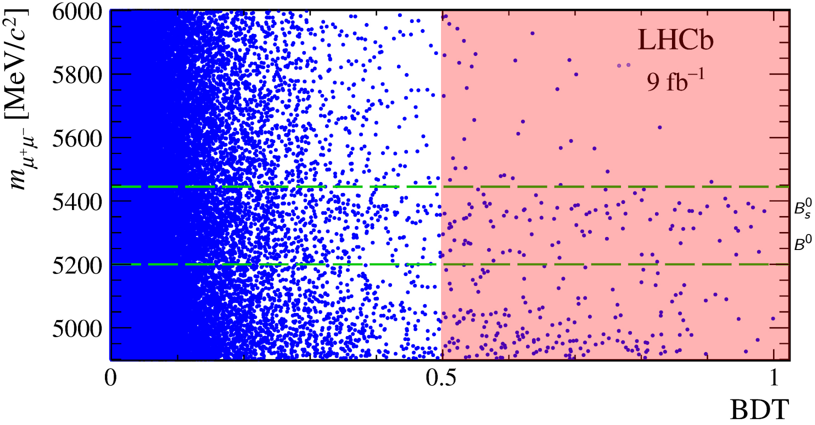

$B \to \mu^+\mu^-$ search using 2011–2018 data ($9\,\text{fb}^{-1}$) is done with a mass fit in bins of BDT output.

[B]

Legacy measurement of $B_s^0 \to \mu^+\mu^-$

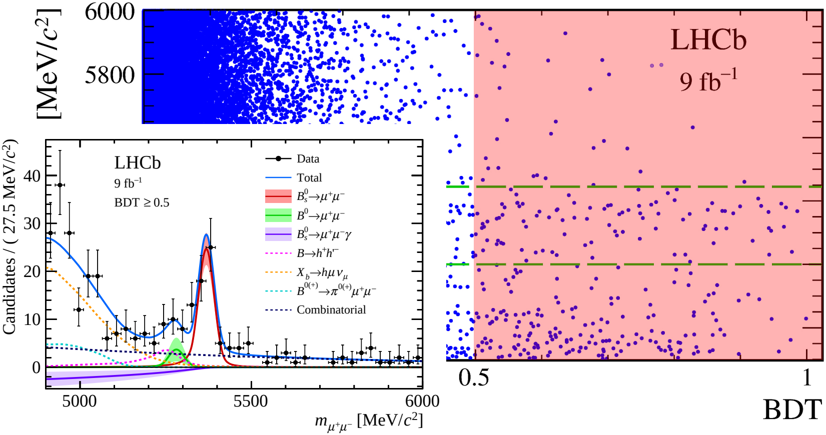

$B \to \mu^+\mu^-$ search using 2011–2018 data ($9\,\text{fb}^{-1}$) is done with a mass fit in bins of BDT output.

[B]

Legacy measurement of $B_s^0 \to \mu^+\mu^-$

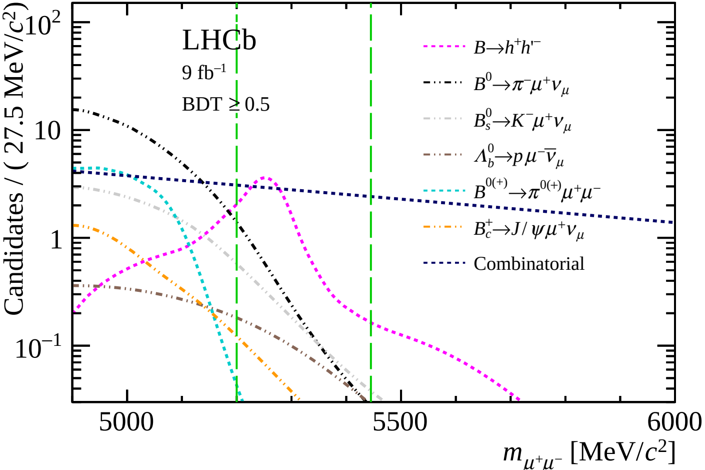

The BDT is optimised to fight combinatorial and specific backgrounds.

Legacy measurement of $B_s^0 \to \mu^+\mu^-$

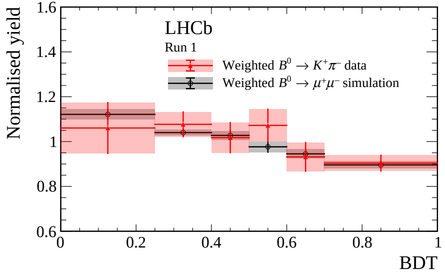

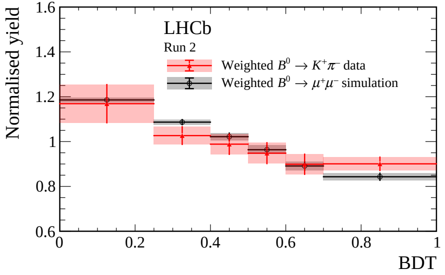

The BDT is calibrated using $B^0 \to K^+\pi^-$ decays, which have the same topology and are more abundant.

Legacy measurement of $B_s^0 \to \mu^+\mu^-$

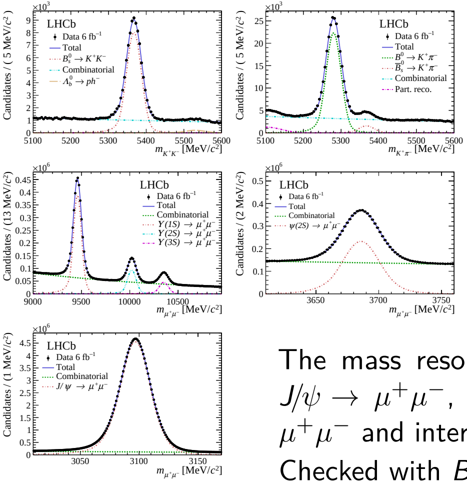

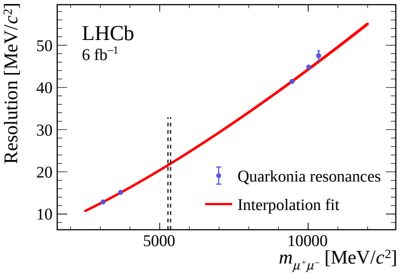

The mass resolution is calibrated using the decays $J/\psi \to \mu^+\mu^-$, $\psi(2S) \to \mu^+\mu^-$ and $\Upsilon([1,2,3]S) \to \mu^+\mu^-$ and interpolated to 23 MeV/c^2 at the B_s^0 mass. Checked with $B^0 \to K^+\pi^-$ and $B_s^0 \to K^+K^-$.

Here for Run 2

[B]

Legacy measurement of $B_s^0 \to \mu^+\mu^-$

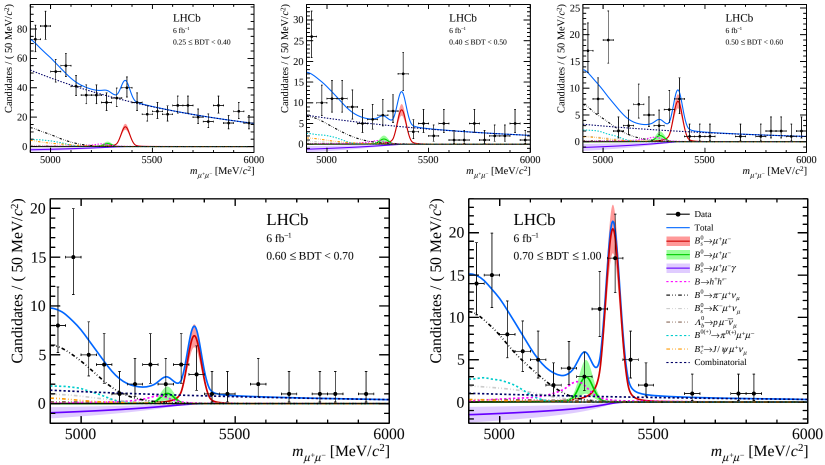

[B]

Mass fits are performed in bins of BDT output, for Run 2.

LEGACY MEASUREMENT OF $B_s^0 \to \mu^+\mu^-$

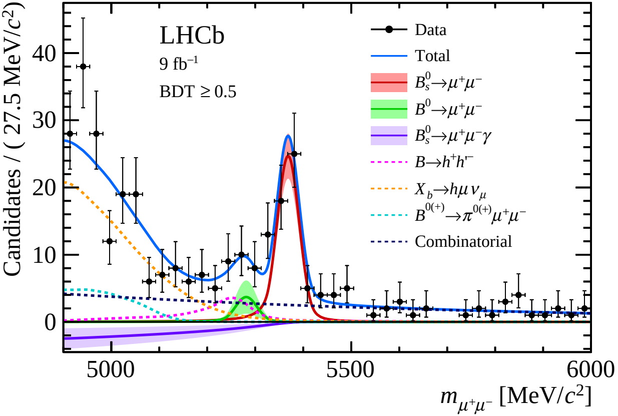

[B] Mass plot shows candidates with BDT> 0.5.

The significances are 10σ for $B_s^0 \to \mu^+\mu^-$ and 1.7σ for $B^0 \to \mu^+\mu^-$.

Legacy measurement of $B_s^0 \to \mu^+\mu^-$

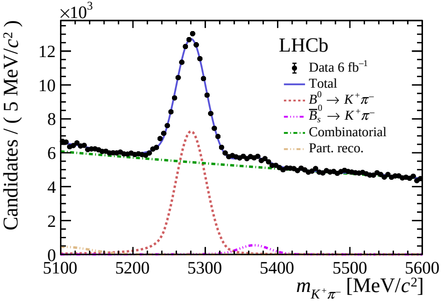

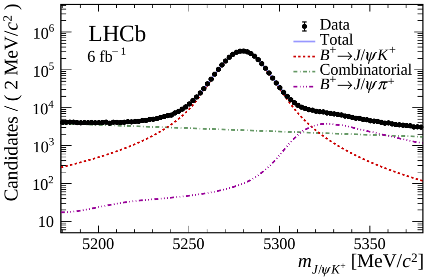

$B^0 \to K^+\pi^-$ and $B^+ \to J/\psi K^+$ are used to normalise the $B \to \mu^+\mu^-$ branching fractions. The factors are $a^{\text{norm}}_{B_s^0\to\mu^+\mu^-} = (2.49 \pm 0.09) \times 10^{-11}$ and $a^{\text{norm}}_{B^0\to\mu^+\mu^-} = (6.52 \pm 0.11) \times 10^{-12}$.

[B]

➜ Expecting 148±8 $B_s^0 \to \mu^+\mu^-$, 16±1 $B \to \mu^+\mu^-$ and about 3 $B_s^0 \to \mu^+\mu^-\gamma$

Legacy measurement of $B_s^0 \to \mu^+\mu^-$

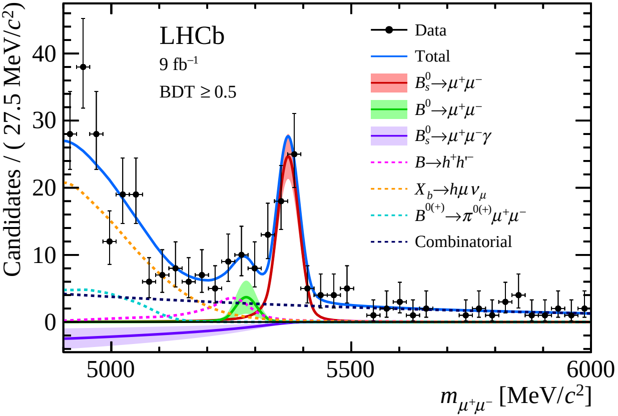

[B] The results $\mathcal{B}(B_s^0 \to \mu^+\mu^-) = (3.09\,^{+\,0.46}_{-\,0.43}\,^{+\,0.15}_{-\,0.11}) \times 10^{-9}$ and $\mathcal{B}(B^0 \to \mu^+\mu^-) = (1.2\,^{+\,0.8}_{-\,0.7} \pm 0.1) \times 10^{-10}$ are consistent with the SM.

Legacy measurement of $B^0_s \to \mu^+\mu^-$

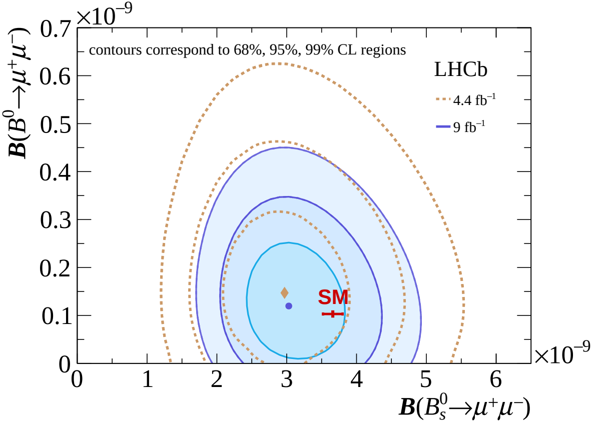

[Beneke, Bobeth, Szafron, JHEP 10 (2019) 232]

The results $\mathcal{B}(B^0_s \to \mu^+\mu^-) = (3.09\,^{+0.46}_{-0.43}\,^{+0.15}_{-0.11}) \times 10^{-9}$ and $\mathcal{B}(B^0 \to \mu^+\mu^-) = (1.2\,^{+0.8}_{-0.7} \pm 0.1) \times 10^{-10}$ are consistent with the SM.

[B]

Legacy measurement of $B_s^0 \to \mu^+\mu^-$

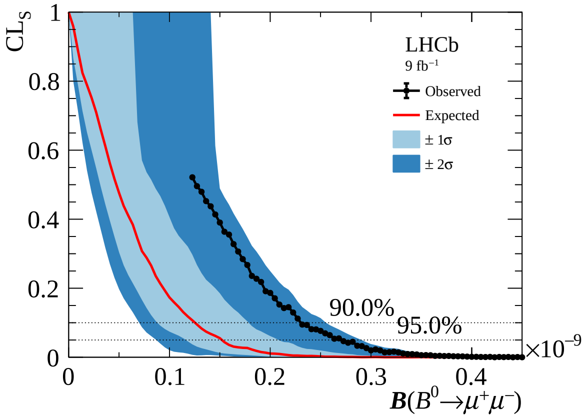

As no excess of $B^0 \to \mu^+\mu^-$ is found, a limit at 2.6×10^{-10} at 95% confidence level is set.

[B]

$B \to \mu^+\mu^-$ WITH 2011–16 DATA

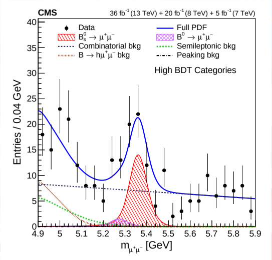

$B_s^0 \to \mu^+\mu^-$ at ATLAS

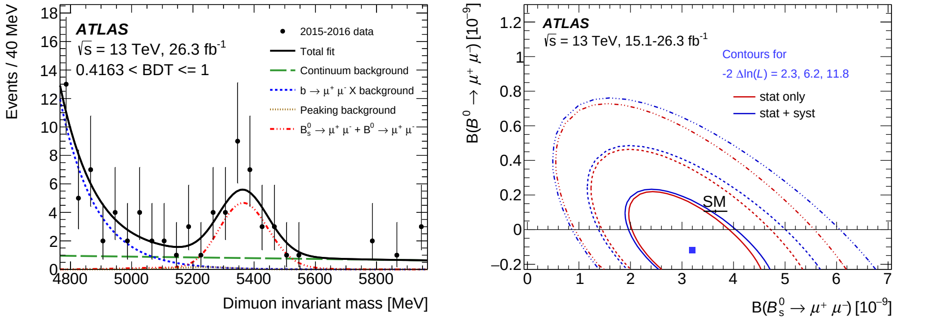

Using 26 fb^{-1} 2015–16 data, ATLAS now also see $B_s^0 \to \mu^+\mu^-$:

$$\mathcal{B}(B_s^0 \to \mu^+\mu^-) = (3.2\,^{+1.0}_{-0.9}\,^{+0.5}_{-0.3}) \times 10^{-9}$$

$$\mathcal{B}(B^0 \to \mu^+\mu^-) = (-1.3 \pm 2.1) \times 10^{-10} < 4.3 \times 10^{-10} \text{ (95\% C.L.)}$$

$B_s^0 \to \mu^+\mu^-$ race toward the SM

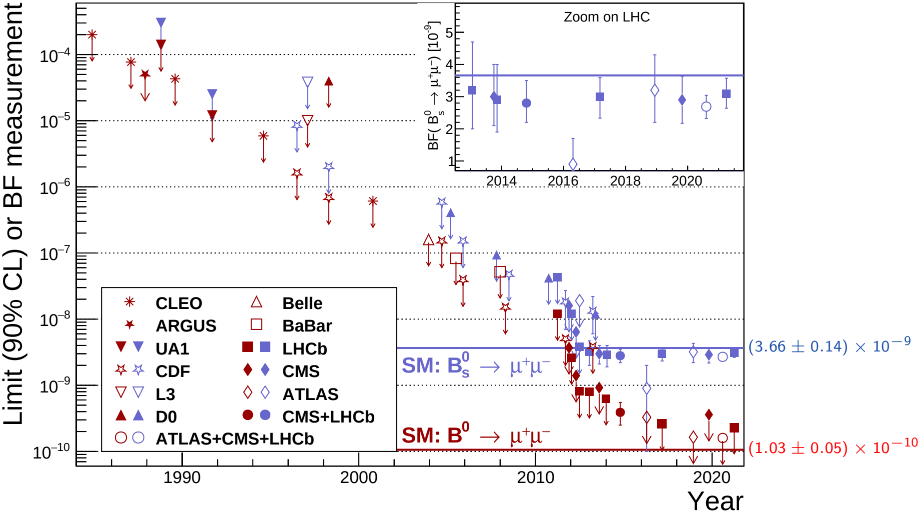

$B \to \mu^+\mu^-$ after Moriond 2021

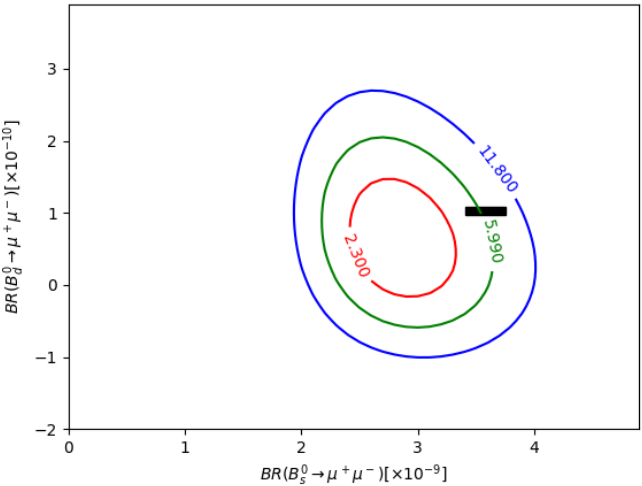

The SM point is near the 2σ band

Buras and Venturini see even 2.7σ using CKM elements from data [Buras, Venturini, arXiv:2203.11960]

ATLAS [JHEP 04 (2019) 098], CMS [JHEP 04 (2020) 188], LHCb [PRL 128 (2022) 041801]

Design of an experiment

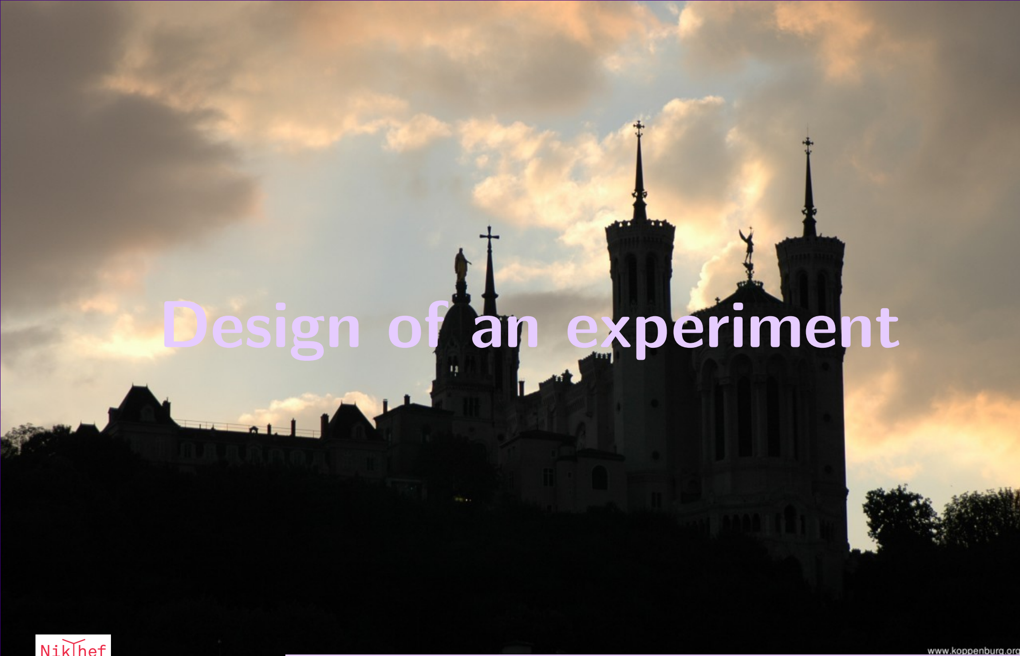

D Lifetime with a microstrip detector

First (?) experiment with a multi-layer silicon microstrip detector

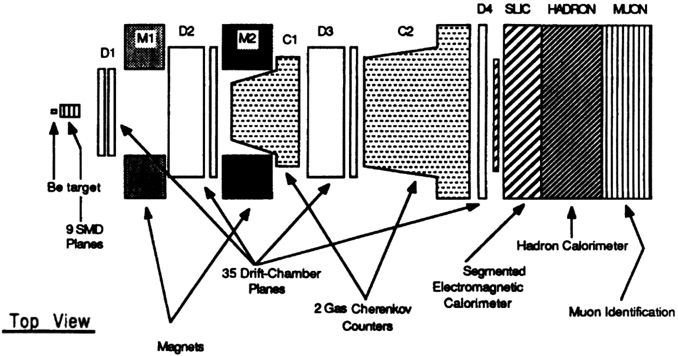

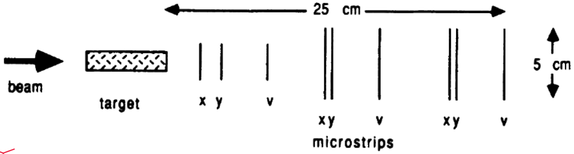

Note the Cherenkov detector

D Lifetime with a microstrip detector

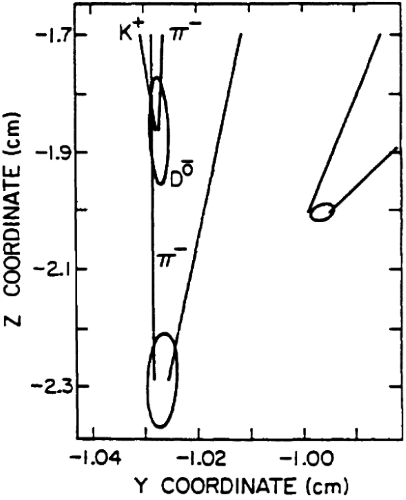

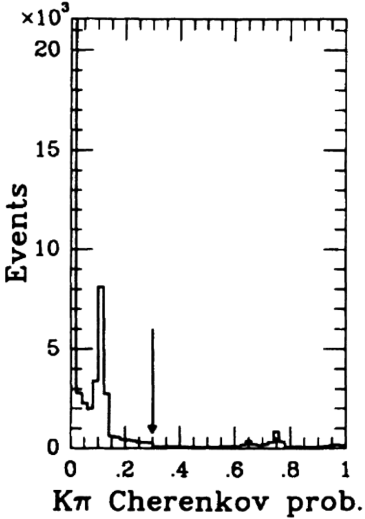

D Lifetime with a microstrip detector

$$\tau_{D^0} = 422 \pm 8 \pm 10\text{ fs} \quad (410.3 \pm 1.0\text{ now})$$
$$\tau_{D^+} = 1090 \pm 30 \pm 25\text{ fs} \quad (1033 \pm 5)$$
$$\tau_{D_s^+} = 470 \pm 40 \pm 20\text{ fs} \quad (504 \pm 4)$$

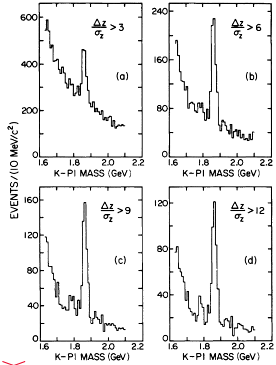

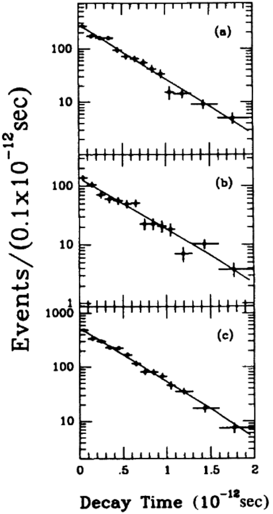

LHCb Legacy 2009–2018

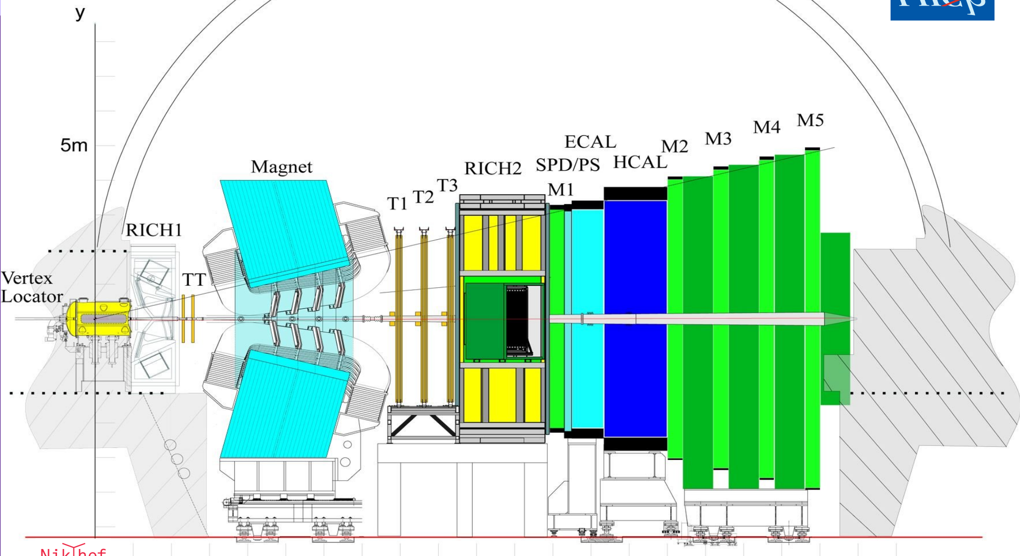

LHCb Upgrade 2023–

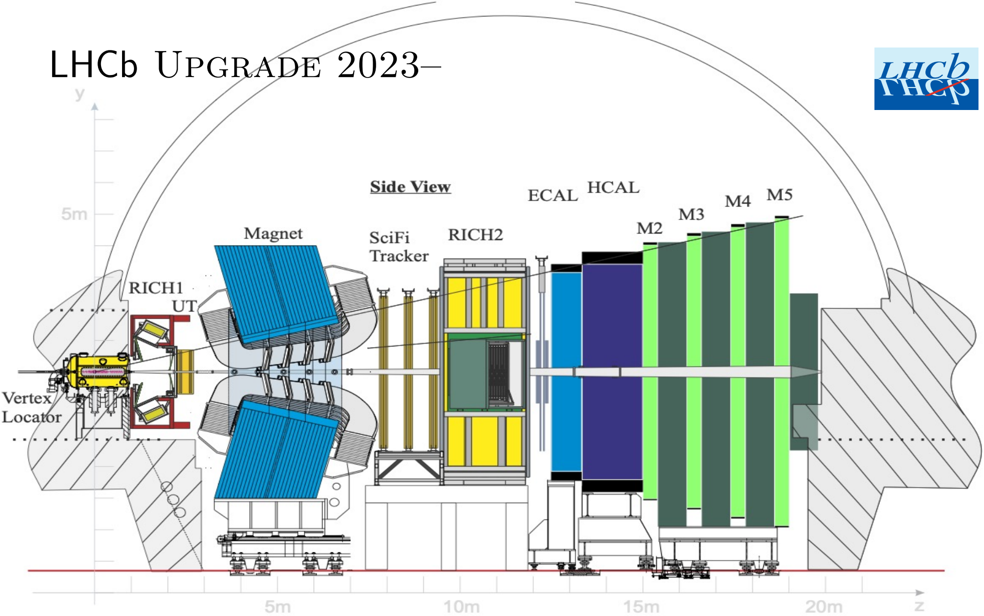

LHCb detector design

Acceptance

Mass and momentum resolution

Impact parameter and time resolution

Particle identification

LHCb detector design: Acceptance

Acceptance: Light particles tend to be closer to the beam pipe. It's cheaper to instrument the forward region than 4π.

$$\ln \frac{\sqrt{s}}{m_X} \geq \eta(X)$$

For Higgs at 13.6 TeV it's 4.7 while for B it's 7.9.

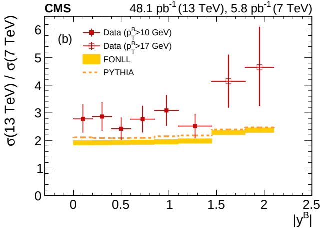

[CMS, PLB 771 (2017) 435]

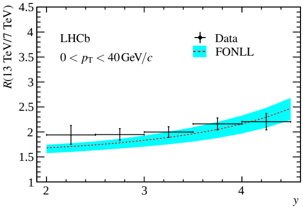

[JHEP 12 (2017) 026]

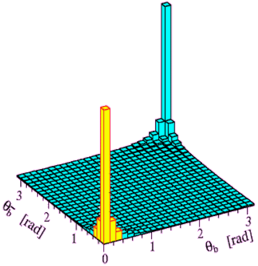

LHCb detector design: Acceptance

Acceptance: Forward

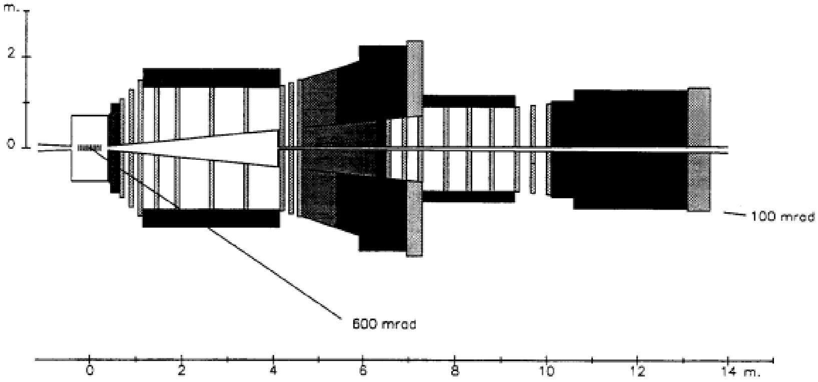

COBEX LOI LHCC-93-50 (1993)

LHCb detector design: Acceptance

Acceptance: Forward

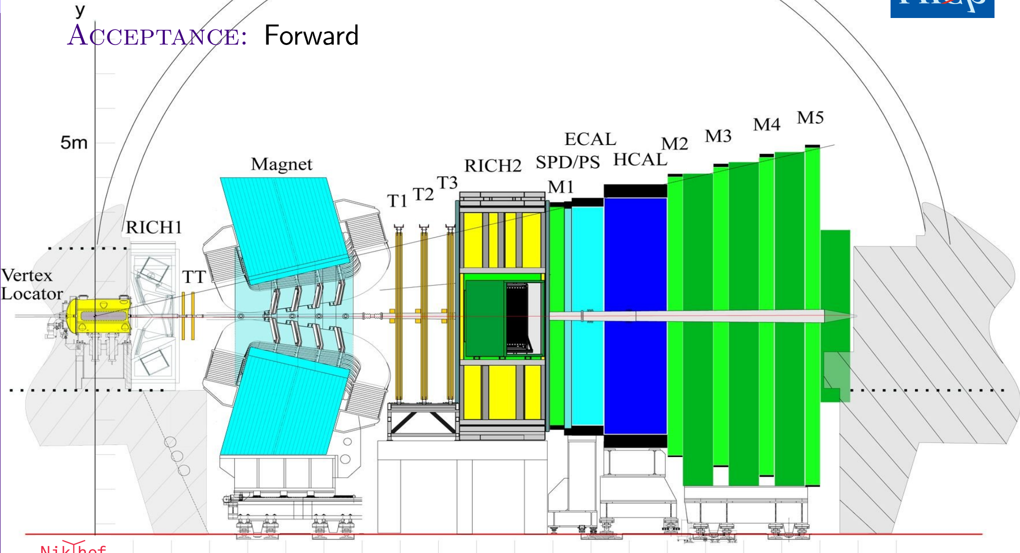

LHCb DETECTOR DESIGN: p RESOLUTION

MASS RESOLUTION: Better resolution translates into better S-B discrimination. But at the minimum we want to resolve the B_s^0 and B^0.

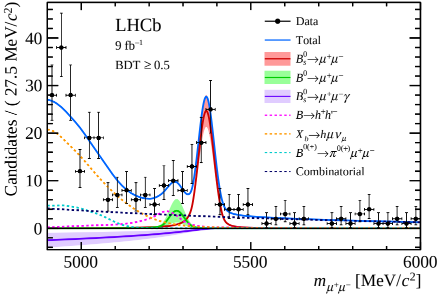

[PRL 128 (2022) 041801]

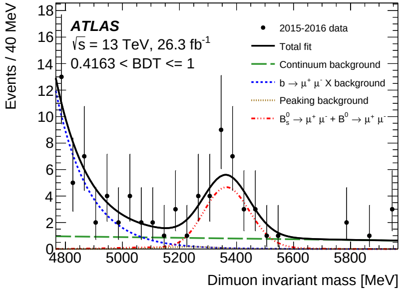

[ATLAS, JHEP 04 (2019) 098]

LHCb DETECTOR DESIGN: p RESOLUTION

MASS RESOLUTION: Better resolution translates into better S-B discrimination. But at the minimum we want to resolve the B_s^0 and B^0.

$$\begin{pmatrix} \sqrt{p_x^2+p_z^2+m^2} \\ p_x \\ 0 \\ p_z \end{pmatrix} = \begin{pmatrix} \sqrt{p_a^2+m_a^2} \\ p_a \\ 0 \\ 0 \end{pmatrix} + \begin{pmatrix} \sqrt{p_b^2+m_b^2} \\ p_b\cos\theta \\ 0 \\ p_b\sin\theta \end{pmatrix}$$

where p_a defines the x direction and y is at an angle θ. This leads to

$$m = \sqrt{m_a^2+m_b^2-2p_ap_b\cos\theta+2\sqrt{m_a^2+p_a^2}\sqrt{m_b^2+p_b^2}}$$

$$\frac{\partial m}{\partial p_a} = \frac{1}{m}\left(p_a\frac{\sqrt{m_b^2+p_b^2}}{\sqrt{m_a^2+p_a^2}} - p_b\cos\theta\right) \qquad \frac{\partial m}{\partial \theta} = \frac{1}{m}p_ap_b\sin\theta$$

LHCb DETECTOR DESIGN: p RESOLUTION

MASS RESOLUTION: Better resolution translates into better S-B discrimination. But at the minimum we want to resolve the B_s^0 and B^0.

$$m = \sqrt{m_a^2 + m_b^2 - 2p_a p_b \cos\theta + 2\sqrt{m_a^2 + p_a^2}\sqrt{m_b^2 + p_b^2}}$$

$$\frac{\partial m}{\partial p_a} = \frac{1}{m}\left(p_a \frac{\sqrt{m_b^2 + p_b^2}}{\sqrt{m_a^2 + p_a^2}} - p_b \cos\theta \right)$$

Plugging in $p_a = p_b = 30\,\text{GeV}$ gets $\theta = 0.18$ for $B_s^0 \to \mu^+\mu^-$

- 3σ B_s^0-B^0 separation ➜ $\leq 30\,\text{MeV}$ resolution
- which translates into $\leq 0.55\%$ p resolution.

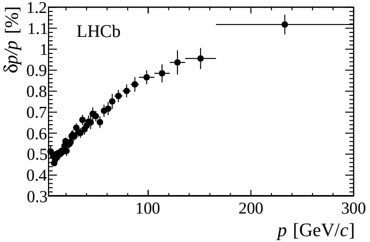

LHCb detector design: p resolution

Mass resolution: Better resolution translates into better S-B discrimination. But at the minimum we want to resolve the B_s^0 and B^0.

➜ Need $\delta p/p \sim 0.5\%$

- In a dipole field the momentum is obtained from the angle of the track before and after the magnet

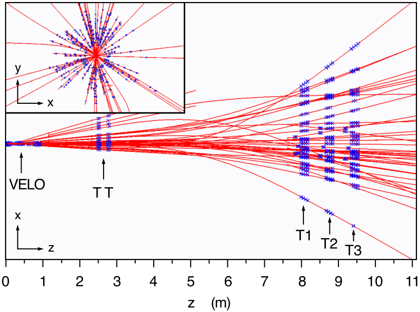

LHCb detector design: p resolution

Mass resolution: Better resolution translates into better S-B discrimination. But at the minimum we want to resolve the B_s^0 and B^0.

➜ Need $\delta p/p \sim 0.5\%$

- In a dipole field the momentum is obtained from the angle of the track before and after the magnet

$$\Delta\vec{p} = p\Delta t_{\mathrm{T}} \qquad t_{\mathrm{T}} = l_{\mathrm{T}}/l_z \qquad \rightarrow \quad \frac{\sigma_p}{p} \simeq \frac{\sigma_{l_{\mathrm{T}}}}{l_{\mathrm{T}}}$$

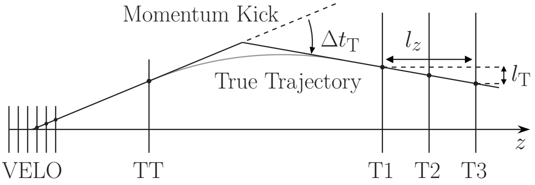

Many handles

1. Hit resolution ➜ $\sigma_{l_{\mathrm{T}}}$
2. Tracking volume l_z
3. B field, and
4. level-arm z ➜ Δt_{T} ➜ $\frac{l_{\mathrm{T}}}{l_z}$

Legacy LHCb: $\sigma_{l_{\mathrm{T}}} \sim 200\,\mu\mathrm{m}$, $l_z \sim 2\,\mathrm{m}$, $\int B \mathrm{d}l_z = 4\,\mathrm{Tm}$

LHCb DETECTOR DESIGN: p RESOLUTION

MASS RESOLUTION: Better resolution translates into better S-B discrimination. But at the minimum we want to resolve the B_s^0 and B^0.

➜ Need $\delta p/p \sim 0.5\%$

- In a dipole field the momentum is obtained from the angle of the track before and after the magnet
- In the upgraded LHCb the SciFi provides 100 μm resolution

[LHCb-DP-2022-002, arXiv:2305.10515]

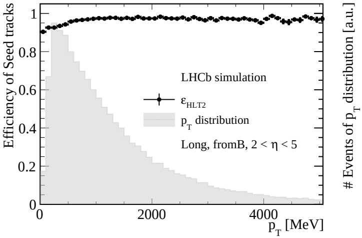

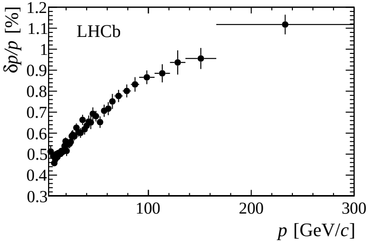

Lifetimes and widths of selected particles

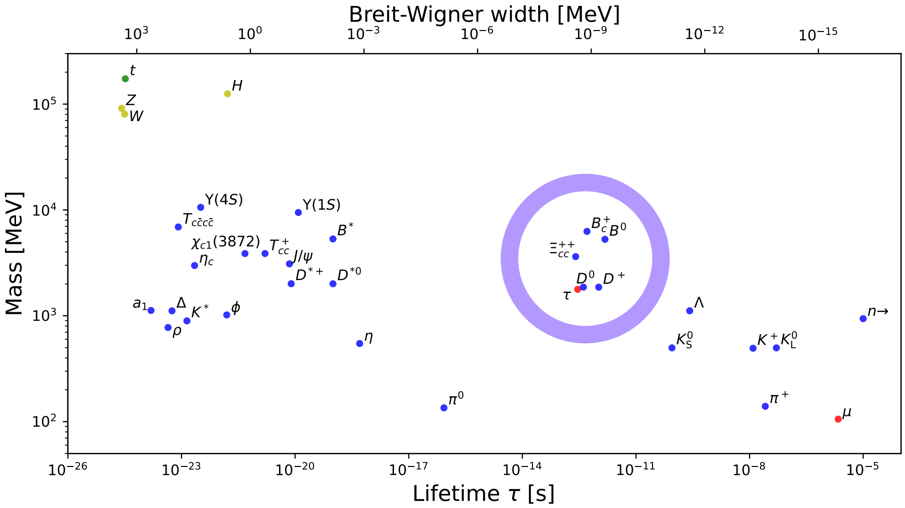

LHCb detector design: Impact parameter

Impact parameter is critical to remove background from prompt tracks

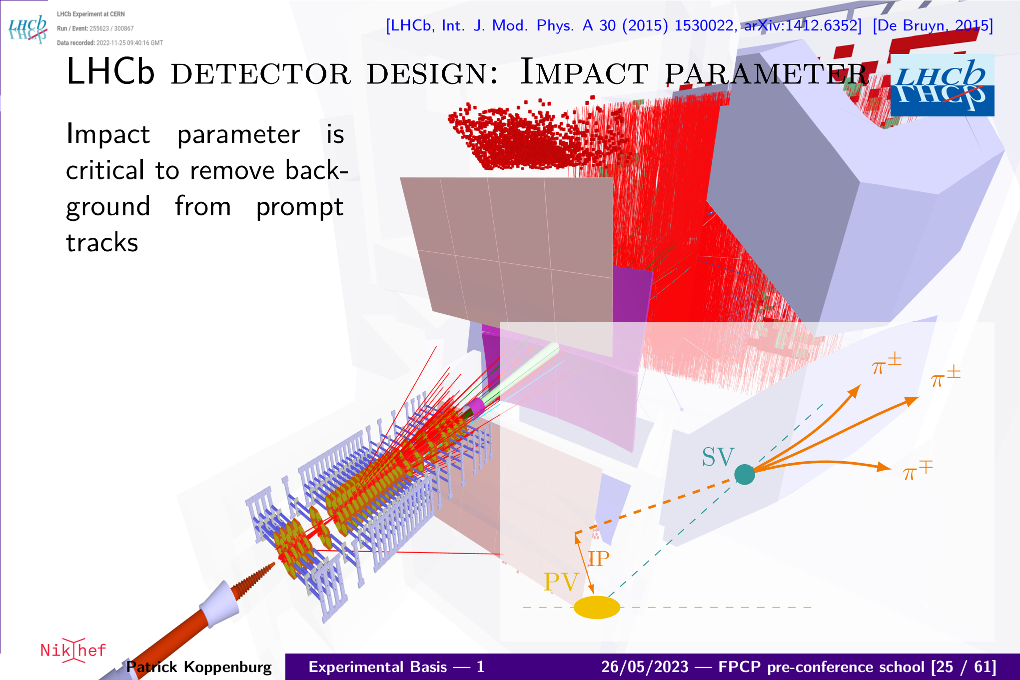

[LHCb, Int. J. Mod. Phys. A 30 (2015) 1530022, arXiv:1412.6352] [De Bruyn, 2015]

LHCb detector design: Impact parameter

Impact parameter is critical to remove background from prompt tracks

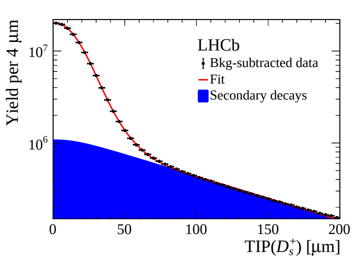

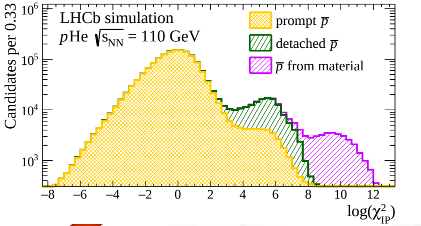

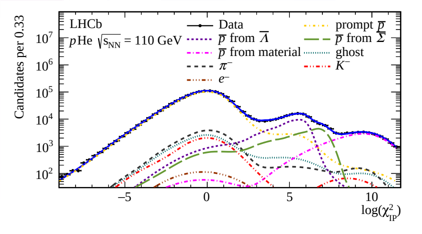

[LHCb, Int. J. Mod. Phys. A 30 (2015) 1530022, arXiv:1412.6352] [De Bruyn, 2015]

LHCb detector design: Impact parameter

IP resolution depends on "track resolution" and "PV resolution", which depends on "track resolution" for N tracks.

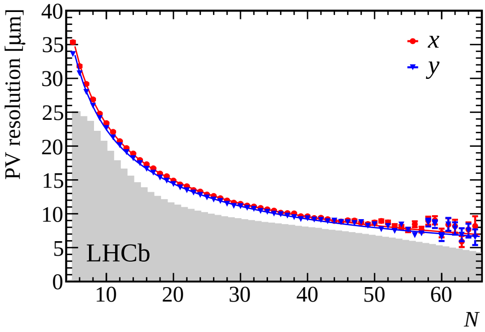

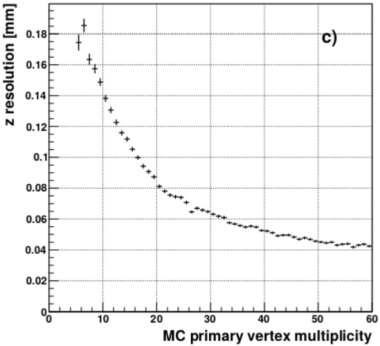

LHCb detector design: Impact parameter

IP is the length of the $\vec{\mathrm{IP}}$ vector. Let's look at x component

$$\mathrm{IP}_x = x - x_{\mathrm{PV}} - (z - z_{\mathrm{PV}})t_x$$

where t_x is the slope of the track in x

$$\sigma^2_{\mathrm{IP_x}} = \sigma^2_x + \sigma^2_{x_{\mathrm{PV}}} + t^2_x\sigma^2_{z_{\mathrm{PV}}} + (z - z_{\mathrm{PV}})^2\sigma^2_{t_x}$$

The last term dominates due to multiple scattering.

$$(z - z_{\mathrm{PV}}) \propto 1/t \qquad \text{(Geometry)}$$

$$\sigma_t \propto 1/p \qquad \text{(Mult. Scat.)}$$

$$\frac{1}{t}\frac{1}{p} = \frac{1}{p_{\mathrm{T}}}$$

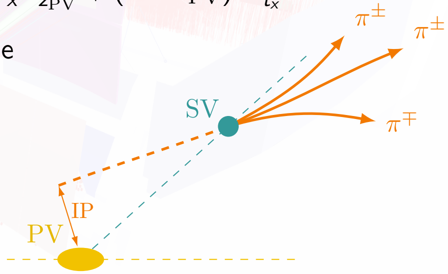

LHCb detector design: Impact parameter

IP is the length of the $\vec{\mathrm{IP}}$ vector. Let's look at x component

$$\mathrm{IP}_x = x - x_{\mathrm{PV}} - (z - z_{\mathrm{PV}})t_x$$

where t_x is the slope of the track in x

$$\sigma^2_{\mathrm{IP_x}} = \sigma^2_x + \sigma^2_{x_{\mathrm{PV}}} + t_x^2\sigma^2_{z_{\mathrm{PV}}} + (z - z_{\mathrm{PV}})^2\sigma^2_{t_x}$$

The last term dominates due to multiple scattering.

$$(z - z_{\mathrm{PV}}) \propto 1/t \quad \text{(Geometry)}$$

$$\sigma_t \propto 1/p \quad \text{(Mult. Scat.)}$$

$$\frac{1}{t}\frac{1}{p} = \frac{1}{p_{\mathrm{T}}}$$

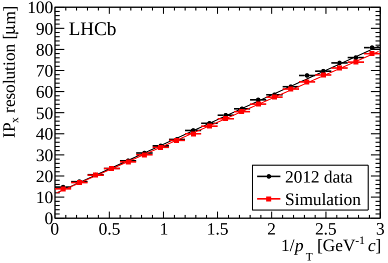

LHCb DETECTOR DESIGN: DECAY TIME

One infers the **decay time** $\boldsymbol{t}$ of a given candidate particle from the measured **flight distance** $\boldsymbol{l}$

$$ct = \gamma l$$

It follows a decaying exponential. The **lifetime** $\boldsymbol{\tau}$ of a particle is the average decay time.

Ω_c^0 LIFETIME HISTORY

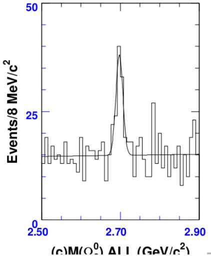

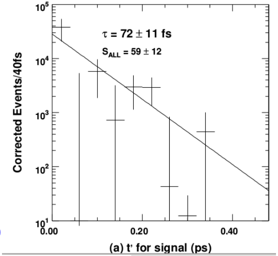

In 2005 FOCUS measure FOCUS measure $72 \pm 11 \pm 11$ fs with 64 ± 14 baryons (resolution: 50 fs) [PLB561 (2003) 41]

In 2018 LHCb get $268 \pm 24 \pm 10 \pm 2$ fs with 978 ± 60 and a resolution of 0.1 fs [LHCb, PRL 121 (2018) 092003, arXiv:1807.02024]

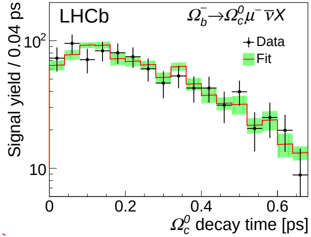

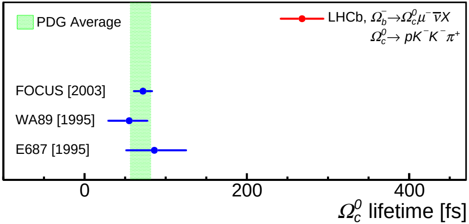

Ω_c^0 LIFETIME HISTOR

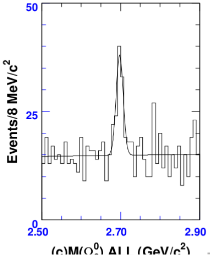

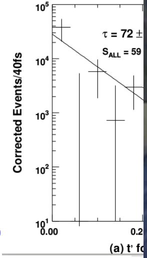

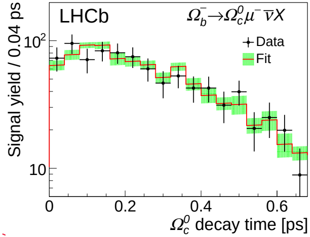

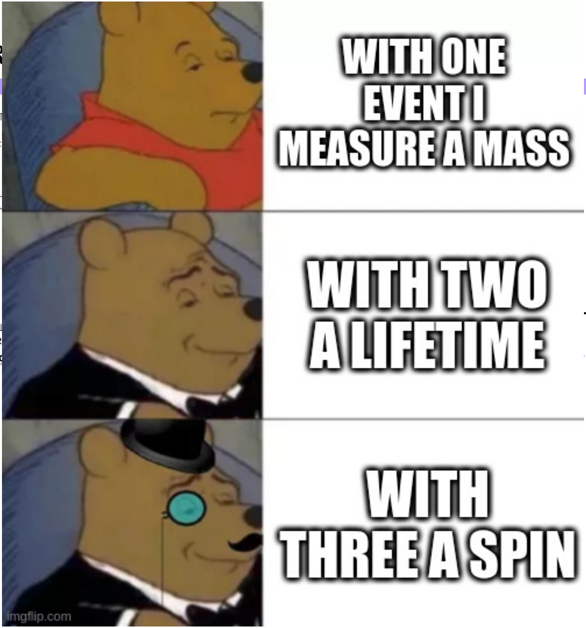

Neutral meson mixing

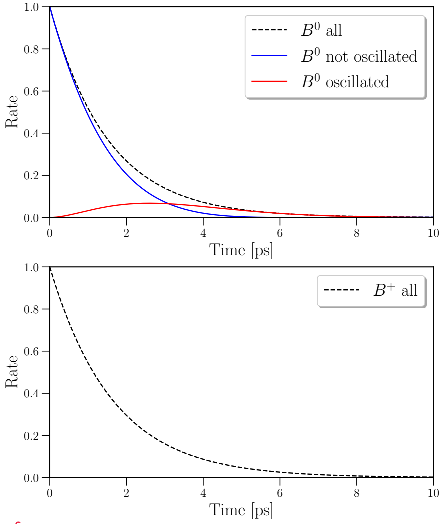

Weakly decaying neutral mesons will exhibit mixing. The two flavour eigentates M and $\overline{M}$ will mix into a heavy M_H and a light M_L state

$$|M_{\mathsf{L,H}}\rangle = p\,|M\rangle \pm q\,\left|\overline{M}\right\rangle .$$

They will oscillate between M and $\overline{M}$ and decay following the lifetimes of M_H and M_L.

Neutral meson mixing

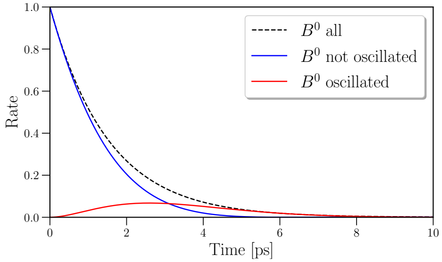

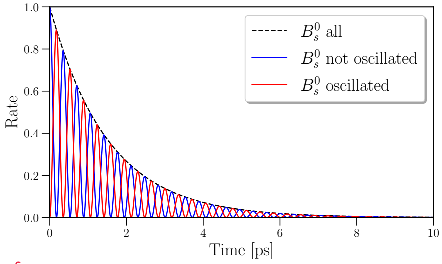

Weakly decaying neutral mesons will exhibit mixing. The two flavour eigentates M and $\overline{M}$ will mix into a heavy M_H and a light M_L state

$$|M_\mathrm{L,H}\rangle = p\,|M\rangle \pm q\,\left|\overline{M}\right\rangle .$$

They will oscillate between M and $\overline{M}$ and decay following the lifetimes of M_H and M_L.

The B_s^0 goes considerably faster than the B^0

LHCb DETECTOR DESIGN: DECAY TIME

One infers the **decay time t** of a given candidate particle from the measured **flight distance l**

$$ct = \gamma l$$

A better time resolution helps for measuring decay times, but is crucial for resolving oscillations

- The B_s^0 sets the strongest constraints
- $\Delta m_s = 17.8\,\text{ps}^{-1}$
  ➜ $1/\Delta m_s = 56\,\text{fs}$

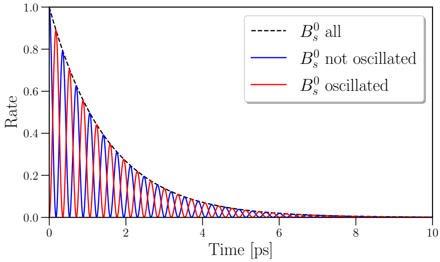

LHCb detector design: decay time

One infers the **decay time t** of a given candidate particle from the measured **flight distance l**

$$ct = \gamma l$$

The resolution is
$$\sigma_t^2 = \left(\frac{m}{p}\right)^2 \sigma_l^2 + \left(\frac{t}{p}\right)^2 \sigma_p^2$$

The resolution σ_l relates to that on IP and PV. At low p multiple scattering dominates. At high p the opening angle is small and detector resolution matters most.

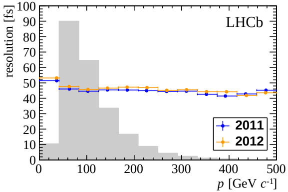

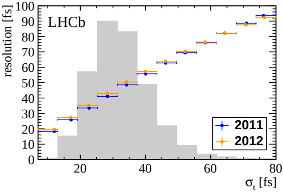

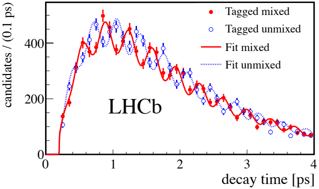

PID

Detector design is imposed by physics. Not much of a choice here.

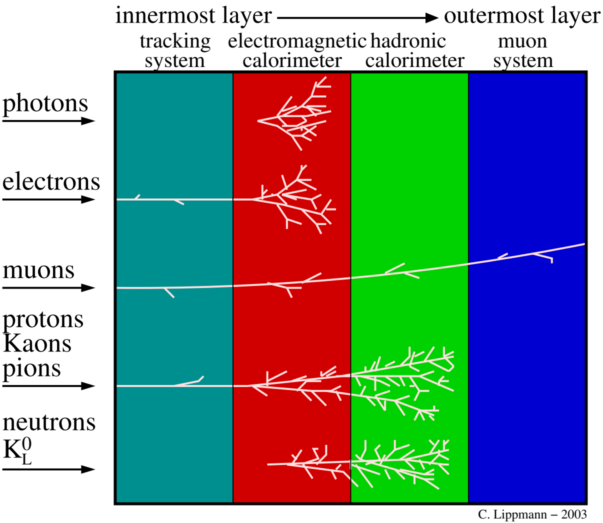

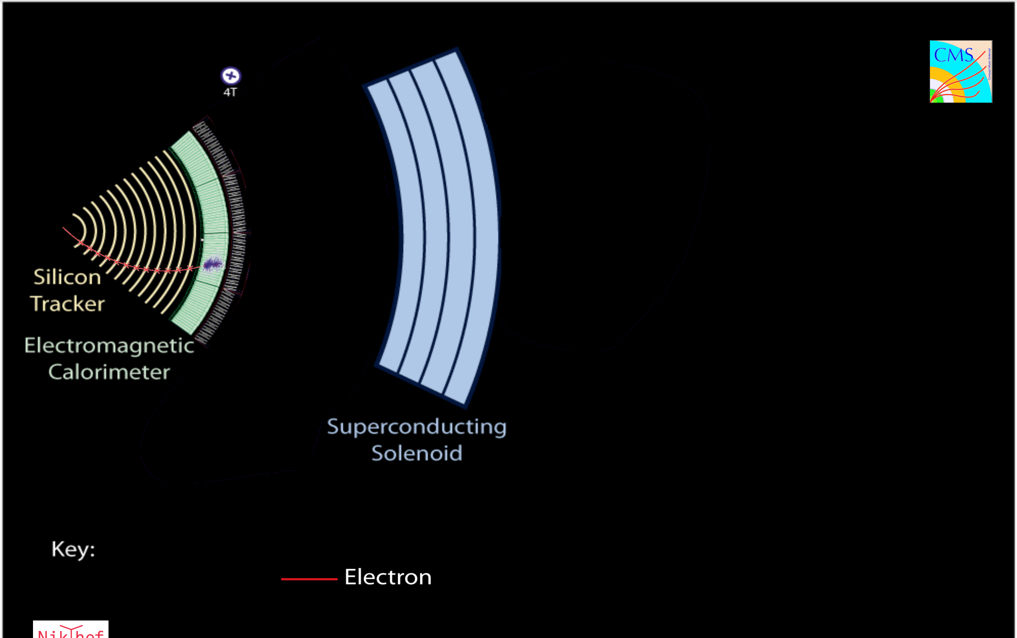
4T
Silicon
Tracker
Electromagnetic
Calorimeter
Superconducting
Solenoid
Key:
Electron
CMS

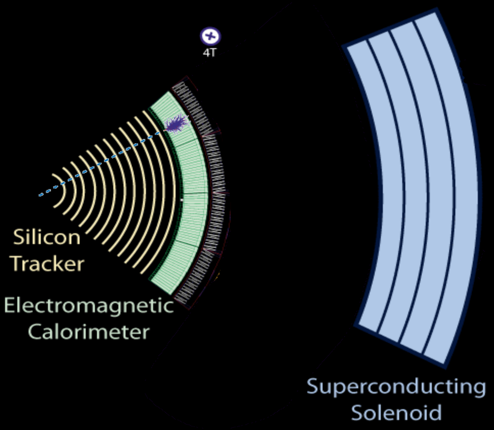
4T
Silicon Tracker
Electromagnetic Calorimeter
Superconducting Solenoid

Key:

- - - - - Photon

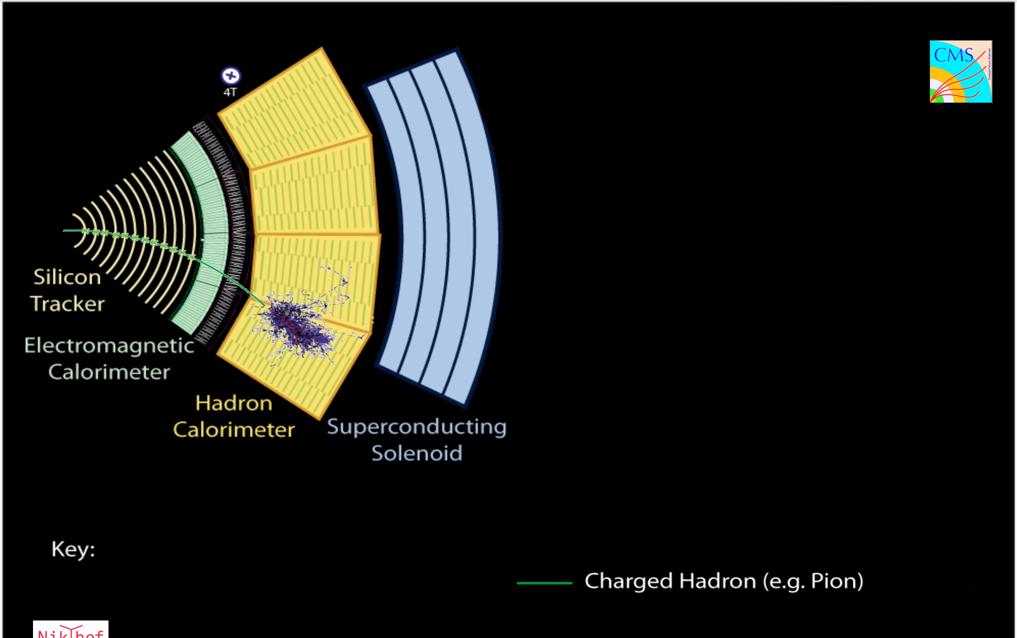
4T
Silicon
Tracker
Electromagnetic
Calorimeter
Hadron
Calorimeter
Superconducting
Solenoid
Key:
Charged Hadron (e.g. Pion)
CMS

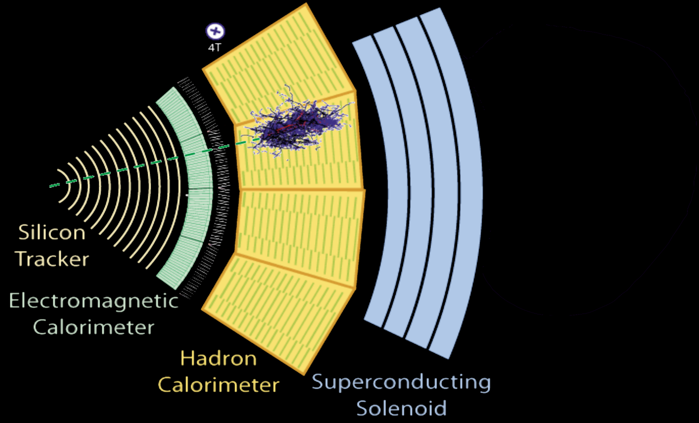

Key:

Neutral Hadron (e.g. Neutron)

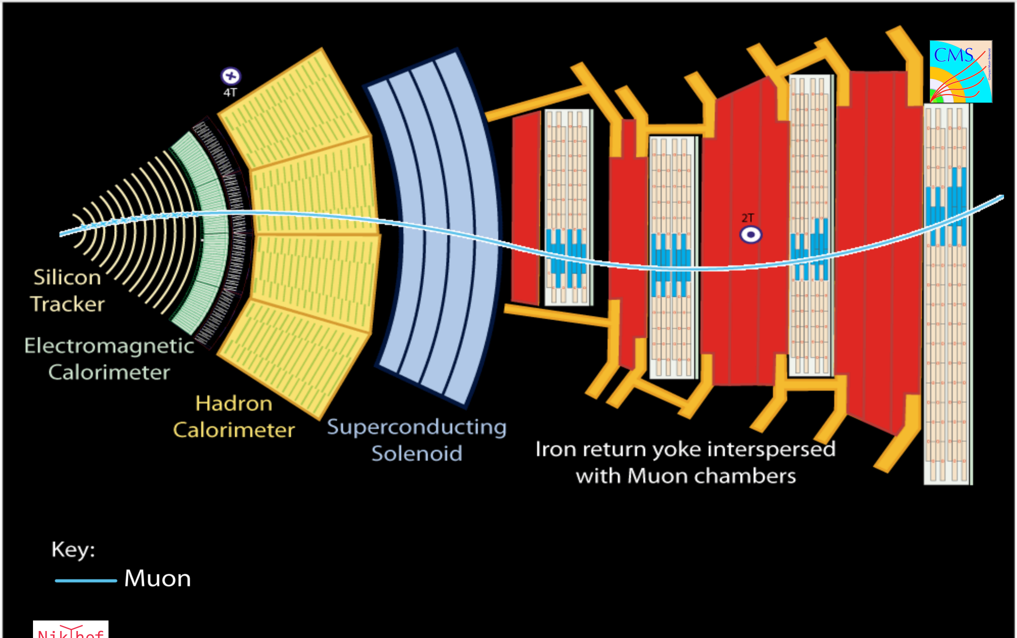
4T
2T
CMS
Silicon Tracker
Electromagnetic Calorimeter
Hadron Calorimeter
Superconducting Solenoid
Iron return yoke interspersed with Muon chambers
Key:
Muon

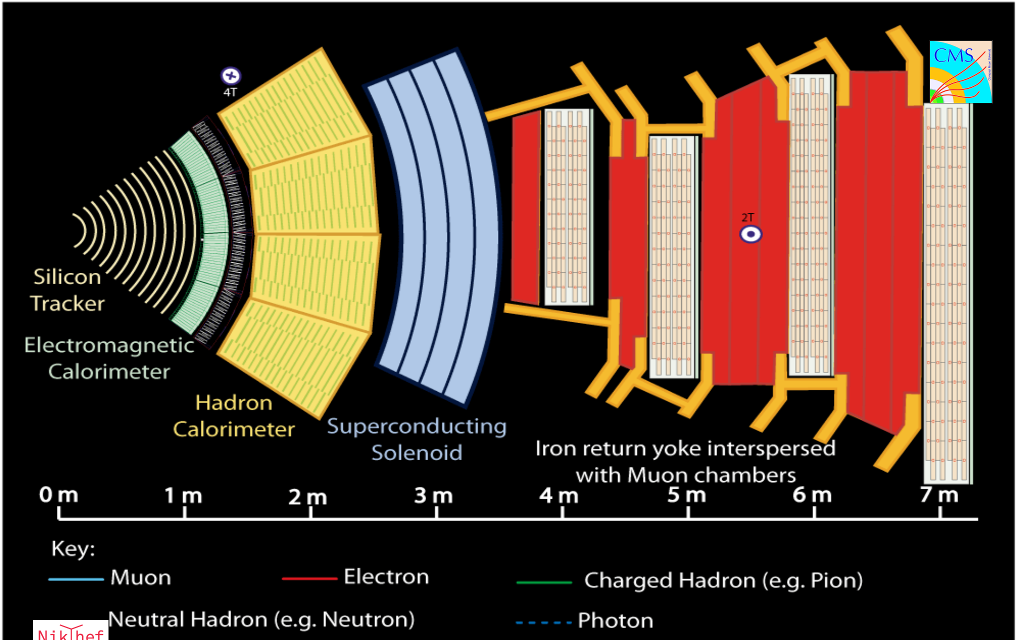
4T
2T
CMS
Silicon Tracker
Electromagnetic Calorimeter
Hadron Calorimeter
Superconducting Solenoid
Iron return yoke interspersed with Muon chambers
0 m
1 m
2 m
3 m
4 m
5 m
6 m
7 m
Key:
Muon
Electron
Charged Hadron (e.g. Pion)
Neutral Hadron (e.g. Neutron)
Photon

LHCb in CMS

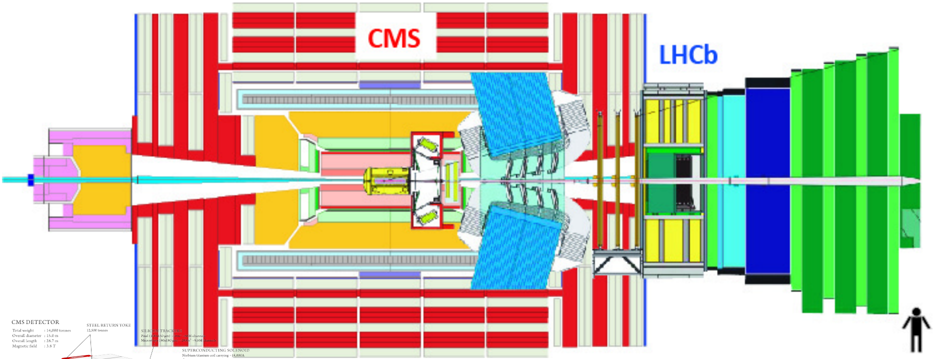
CMS
LHCb

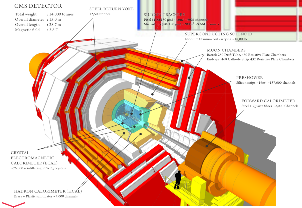
CMS DETECTOR
Total weight : 14,000 tonnes
Overall diameter : 15.0 m
Overall length : 28.7 m
Magnetic field : 3.8 T
STEEL RETURN YOKE
12,500 tonnes
SUPERCONDUCTING SOLENOID
Niobium titanium coil carrying ~18,000A
MUON CHAMBERS
Barrel: 250 Drift Tube, 480 Resistive Plate Chambers
Endcaps: 468 Cathode Strip, 432 Resistive Plate Chambers
PRESHOWER
FORWARD CALORIMETER
Steel + Quartz fibres ~2,000 Channels
CRYSTAL
ELECTROMAGNETIC
CALORIMETER (ECAL)
HADRON CALORIMETER (HCAL)
Brass + Plastic scintillator ~7,000 channels

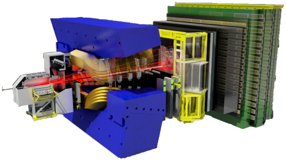

LHCb

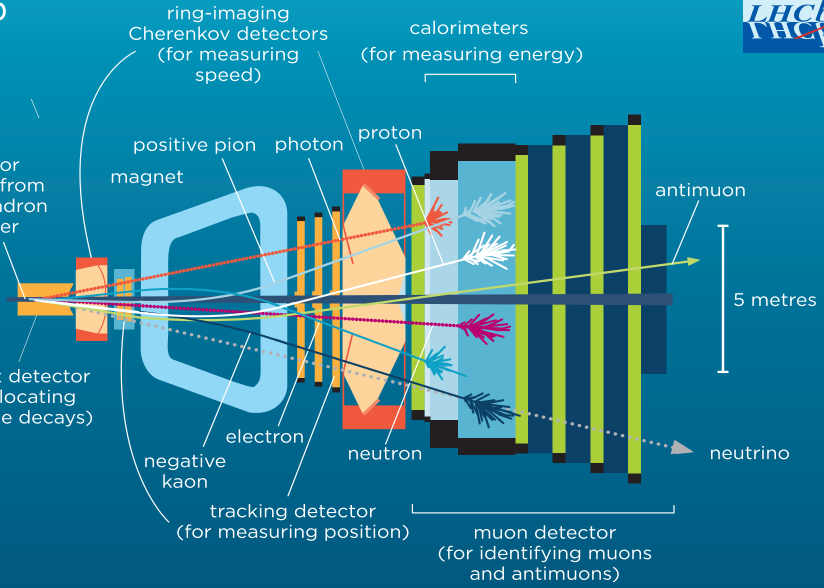
ring-imaging
Cherenkov detectors
(for measuring
speed)
calorimeters
(for measuring energy)
pipe for
protons from
Large Hadron
Collider
positive pion
photon
proton
magnet
antimuon
5 metres
vertex detector
(for locating
particle decays)
electron
neutron
neutrino
negative
kaon
tracking detector
(for measuring position)
muon detector
(for identifying muons
and antimuons)

P_{ψ}^{N+} states at ATLAS

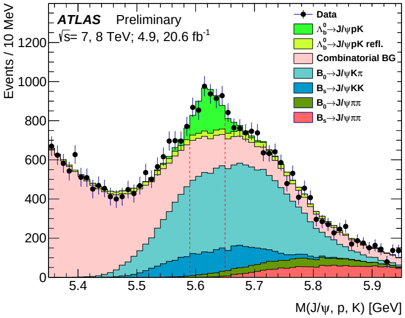

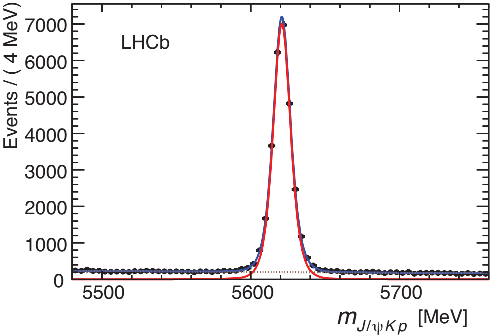

With Run 1 data, ATLAS find 2270 ± 300 $\Lambda_b^0 \to J/\psi p K^-$ decays

- With the same data, LHCb see $26\,000 \pm 170$ with hardly any background

[LHCb, PRL 115 (2015) 072001, arXiv:1507.03414]

[Cherenkov, Dokl.Akad.Nauk SSSR 2 (1934) 8, 451]

Cherenkov

Cherenkov radiation is emitted by charged particles crossing a transparent medium at a speed higher than the speed of light *in that medium*.

$$v = \frac{c}{n}$$

➜ Like boom of a supersonic aircraft.

Cherenkov

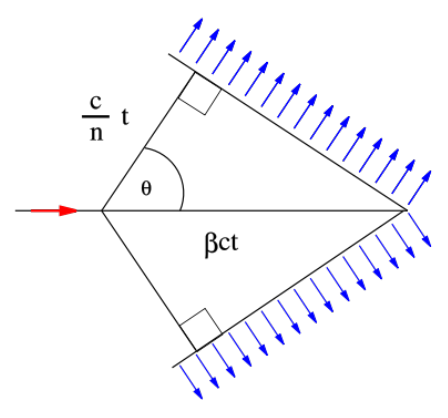

Cherenkov radiation is emitted by charged particles crossing a transparent medium at a speed higher than the speed of light *in that medium*.

$$v = \frac{c}{n}$$

➜ Like boom of a supersonic aircraft.

[Cherenkov, Dokl.Akad.Nauk SSSR 2 (1934) 8, 451]

Cherenkov

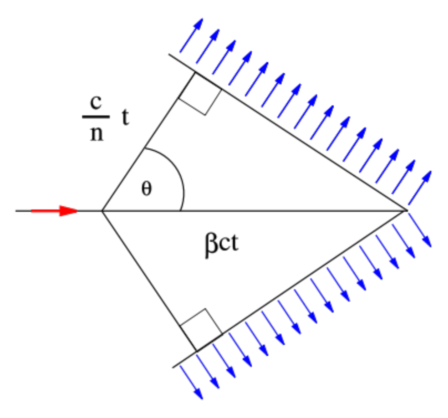

Cherenkov radiation is emitted by charged particles crossing a transparent medium at a speed higher than the speed of light *in that medium*.

$$v = \frac{c}{n}$$

➜ Like boom of a supersonic aircraft.

- The emission angle depends on the speed of the particle.
- From the speed and the momentum one can work out the mass. Hence the identitv

LHCb RICH performance in Run 2

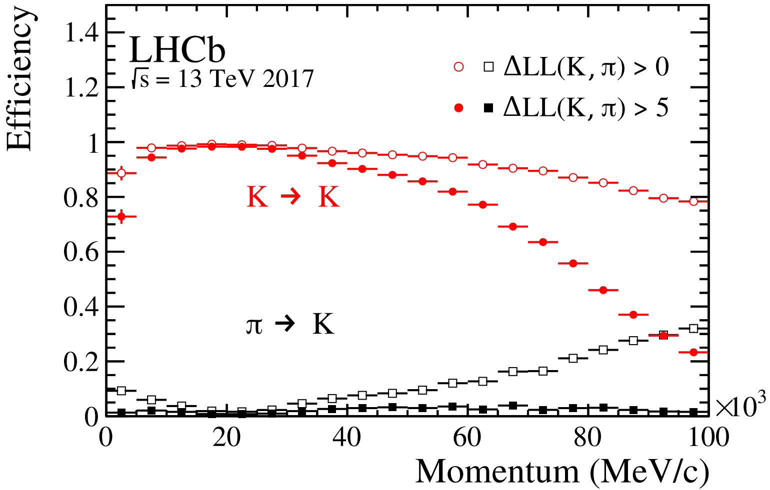

Velo Incident

VELO INCIDENT

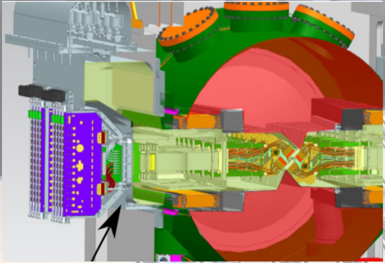

On 10th January 2023, during a VELO warm up in neon, there was a loss of control of the protection system. A pressure differential of 200 mbar built up between the two volumes, whereas the foils are designed to withstand 10 mbar only. Initial investigations show no damage to the VELO modules; sensors show correct leakage currents, microchannels show no leaks.

RF foils have suffered plastic deformation up to 14 mm and have to be replaced.

- Major intervention, planning under study Replace now (delay), or replace at the end of the year (run in 2023 with VELO partially open)
- Physics programme of 2023 is significantly affected, commissioning of Upgrade I systems can proceed as planned

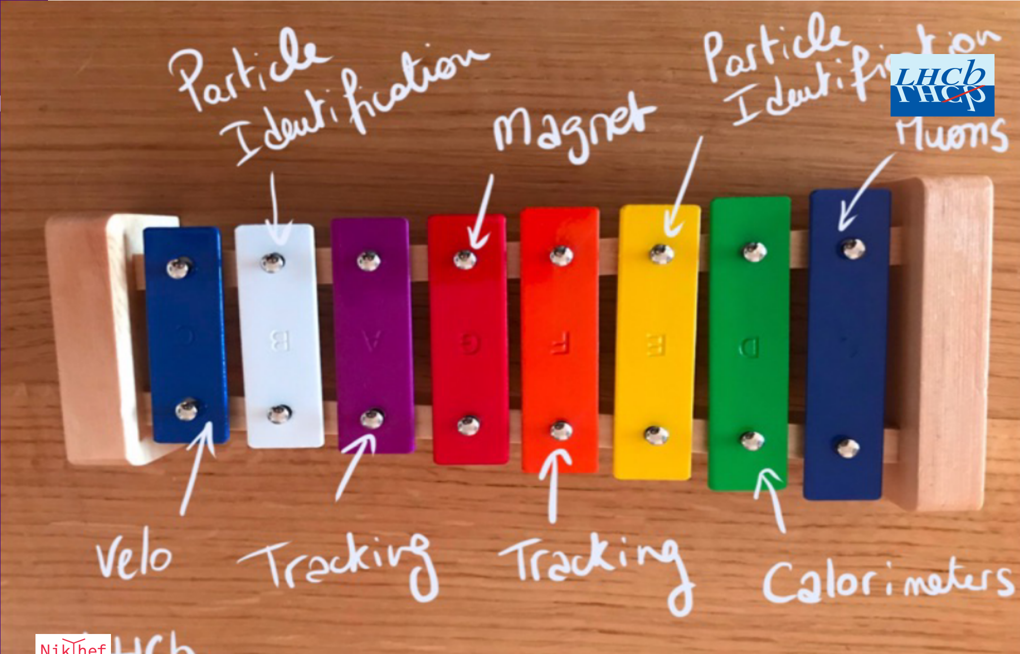
Particle Identification
Magnet
Particle Identification
Muons
Velo
Tracking
Tracking
Calorimeters

LHCb

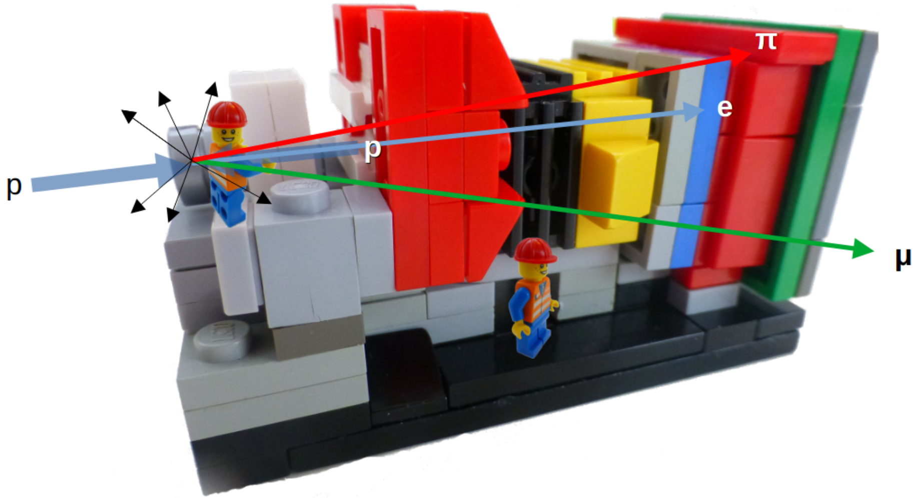

LHCb

LHCb

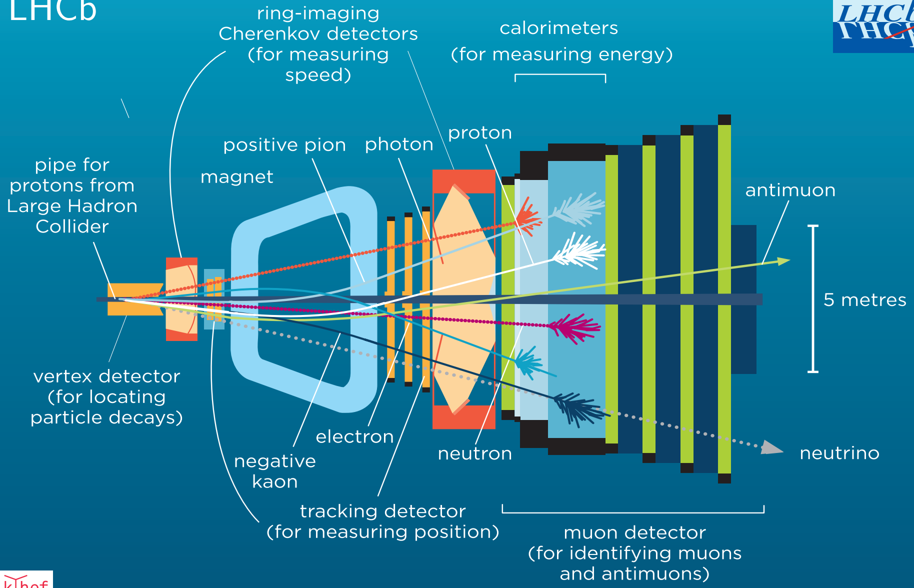
ring-imaging Cherenkov detectors (for measuring speed)
calorimeters (for measuring energy)
pipe for protons from Large Hadron Collider
magnet
positive pion
photon
proton
antimuon
5 metres
vertex detector (for locating particle decays)
electron
negative kaon
neutron
neutrino
tracking detector (for measuring position)
muon detector (for identifying muons and antimuons)

LHCb

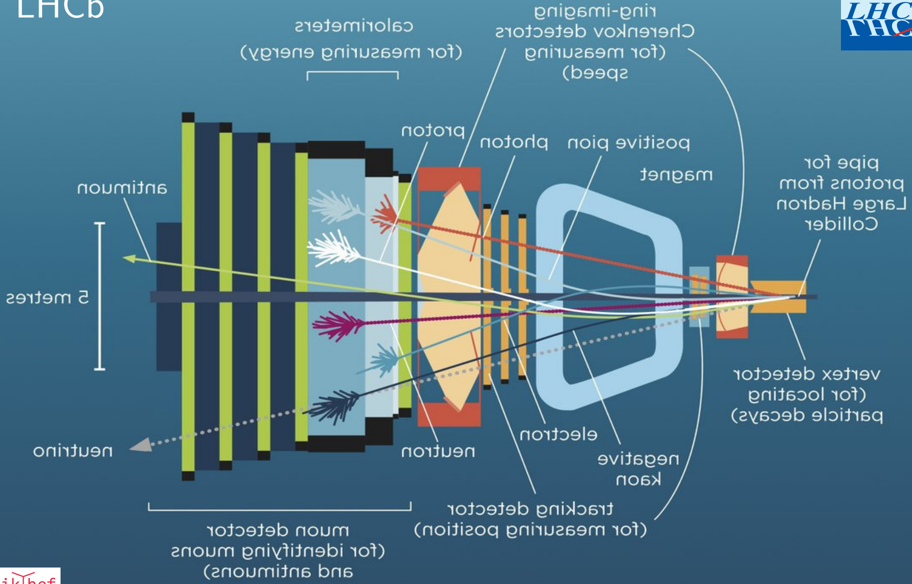
calorimeters
(for measuring energy)
ring-imaging
Cherenkov detectors
(for measuring
speed)
proton
photon
positive pion
magnet
pipe for
protons from
Large Hadron
Collider
antimuon
5 metres
vertex detector
(for locating
particle decays)
neutrino
neutron
electron
negative
kaon
tracking detector
(for measuring position)
muon detector
(for identifying muons
and antimuons)

LHCb

LHCb

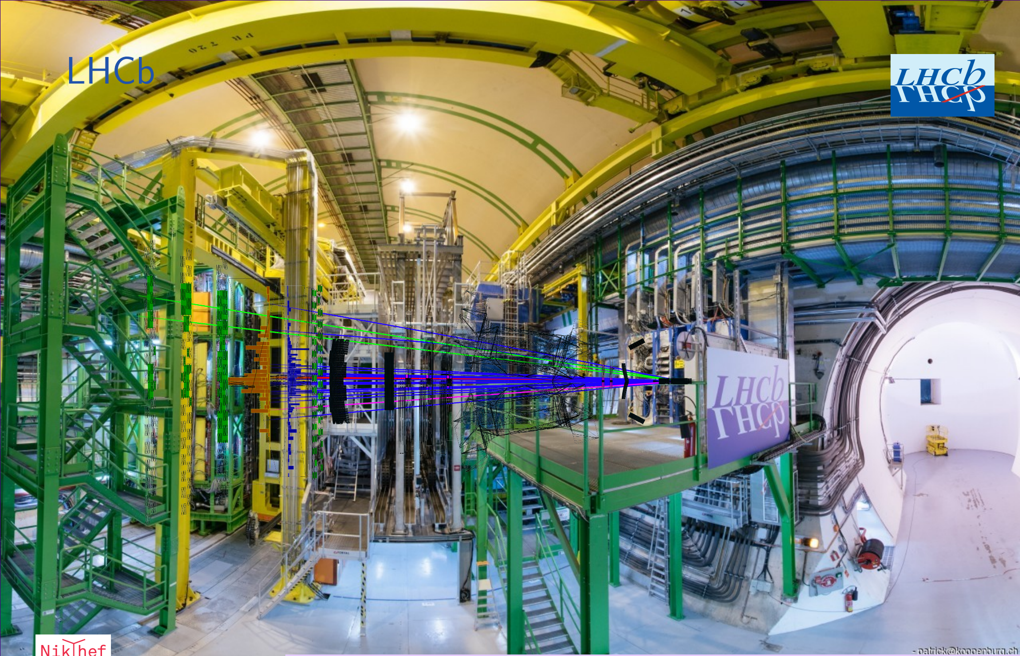

The Large Hadron Collider at CERN

ATLAS

[ATLAS, JINST 3 (2008) S08003]

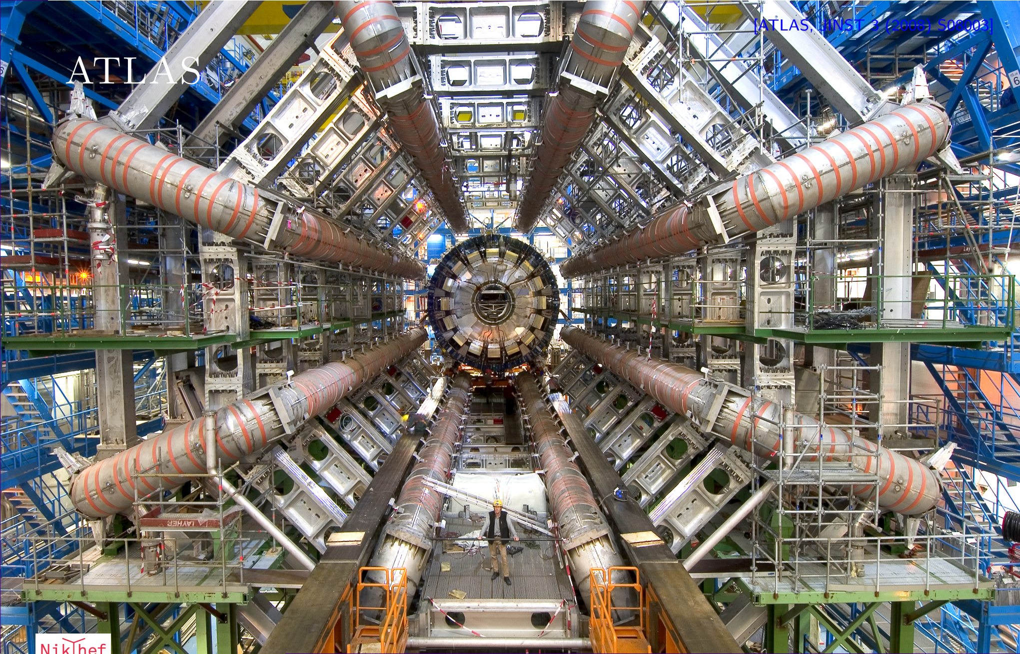

CMS

[CDS]

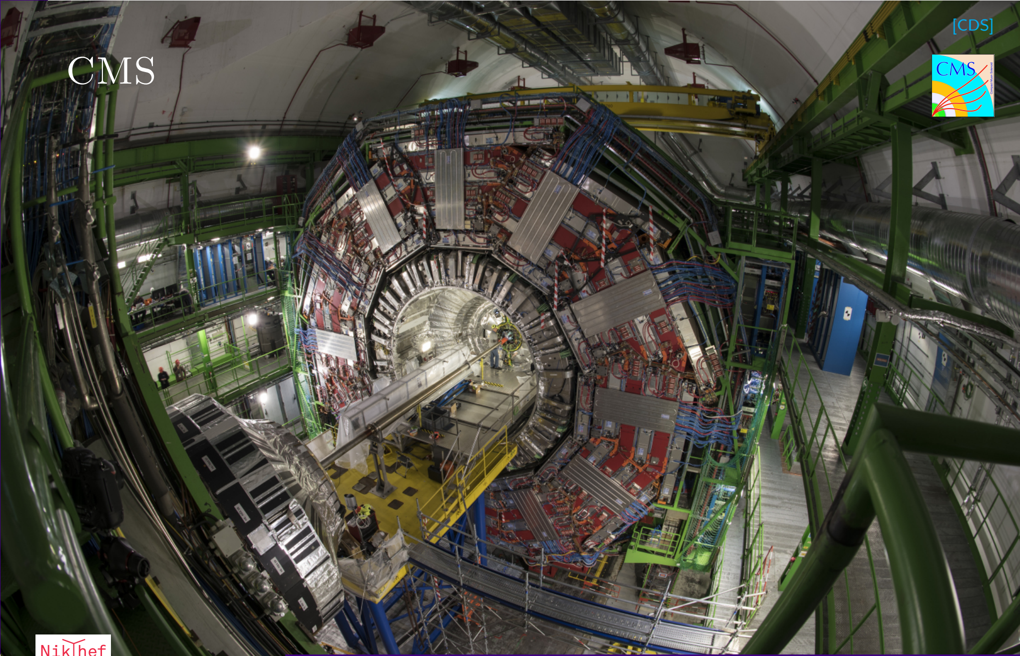

Belle and Belle II

22/09/2022 - CERN

Belle Control Room (2003)

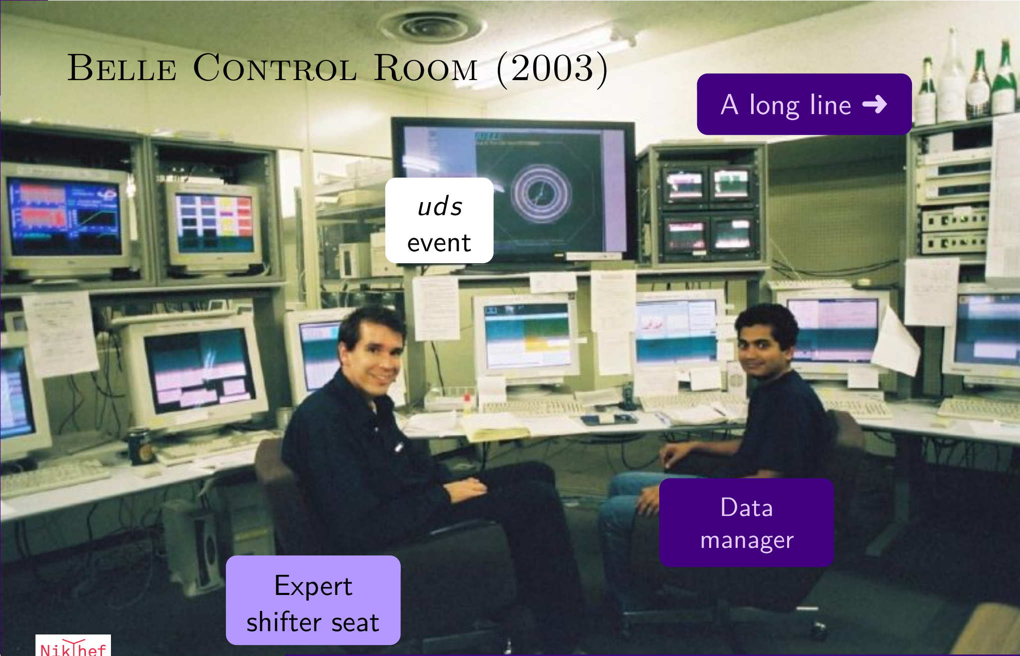

Belle Control Room (2003)

The Belle Experiment

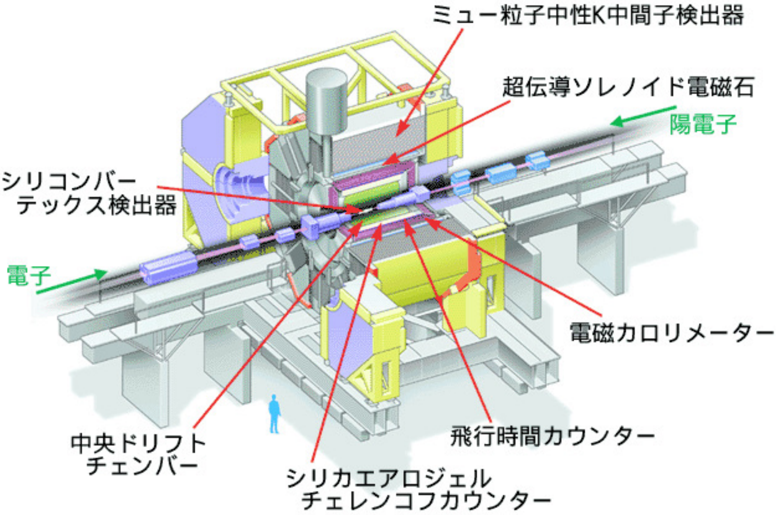

BaBar

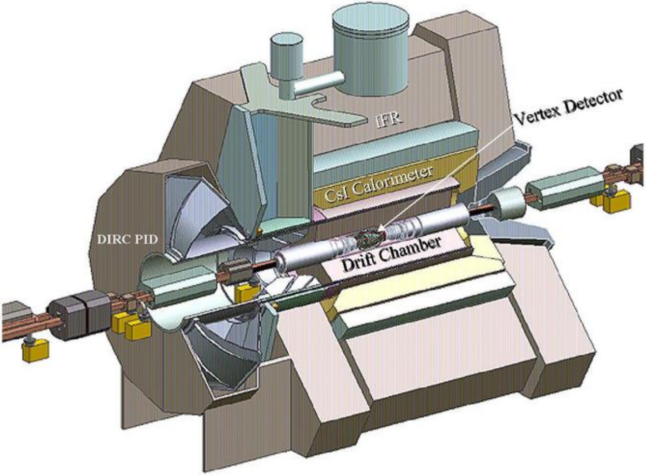

IFR
Vertex Detector
CsI Calorimeter
DIRC PID
Drift Chamber

Belle II

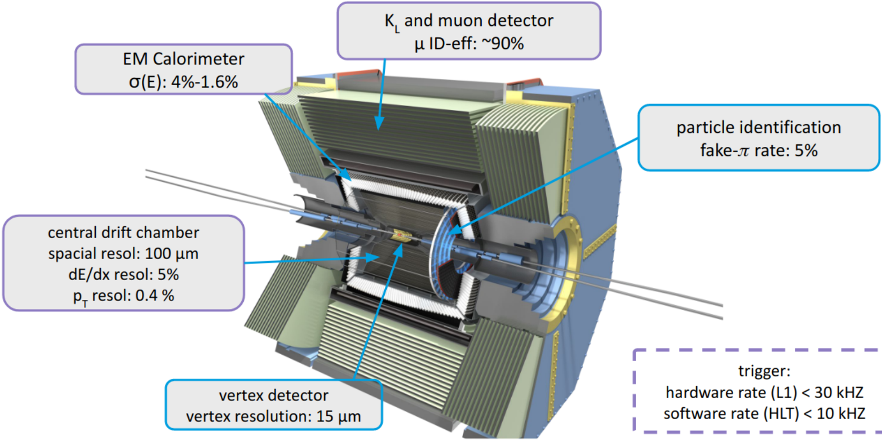

trigger:
hardware rate (L1) < 30 kHZ
software rate (HLT) < 10 kHZ

Belle II

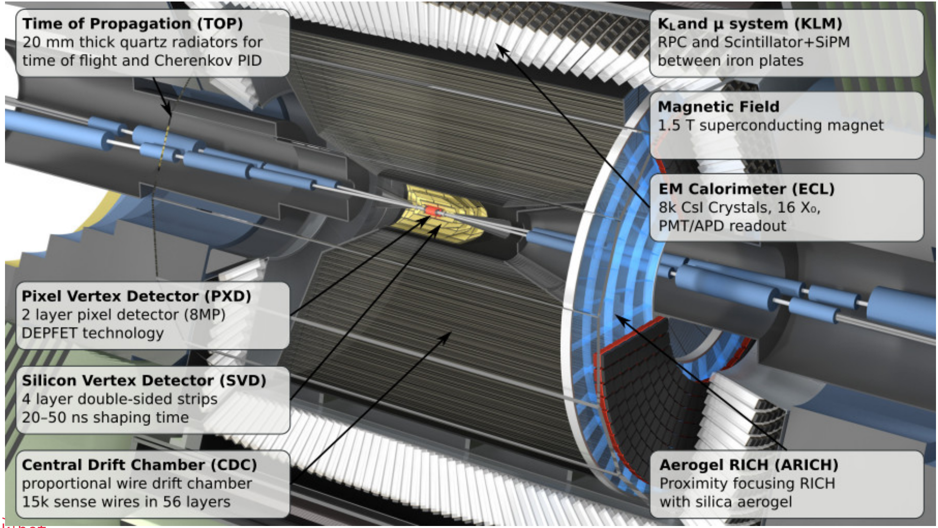
Belle II
Time of Propagation (TOP)
20 mm thick quartz radiators for
time of flight and Cherenkov PID
K_L and μ system (KLM)
RPC and Scintillator+SiPM
between iron plates
Magnetic Field
1.5 T superconducting magnet
EM Calorimeter (ECL)
8k CsI Crystals, 16 X_0,
PMT/APD readout
Pixel Vertex Detector (PXD)
2 layer pixel detector (8MP)
DEPFET technology
Silicon Vertex Detector (SVD)
4 layer double-sided strips
20–50 ns shaping time
Central Drift Chamber (CDC)
proportional wire drift chamber
15k sense wires in 56 layers
Aerogel RICH (ARICH)
Proximity focusing RICH
with silica aerogel

Belle II

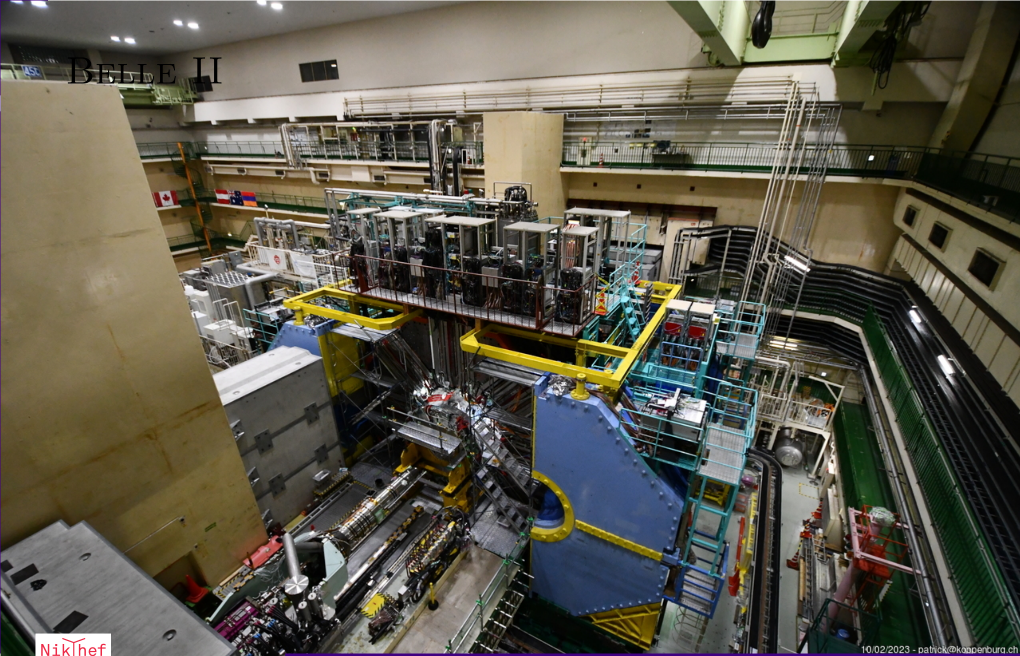

Υ RESONANCES

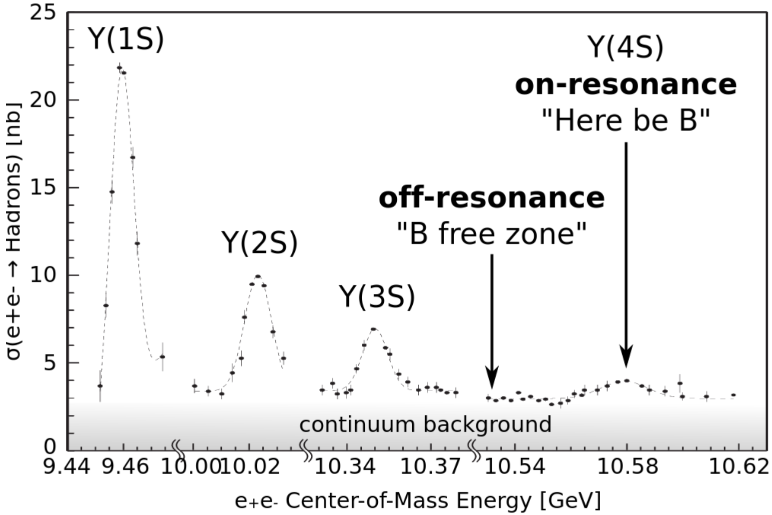

Quantum entanglement

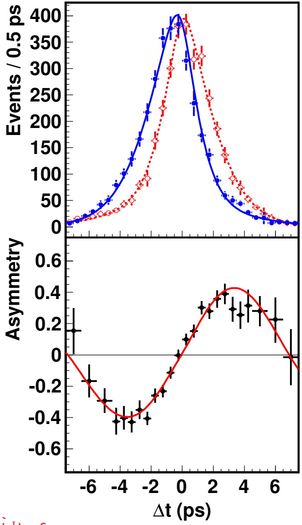

The B^0 and $\bar{B}^0$ originate from a $\Upsilon(4S)$ resonance. They are produced in a quantum-entangled state of a superposition of B^0 and $\bar{B}^0$. The flavour of the one is only fixed once the other decays.

Unlike at the LHC, the clock only starts at the time the other B decays.

➜ The difference in flight time is relevant

- This difference can be negative, if the signal B decays before the tag B.

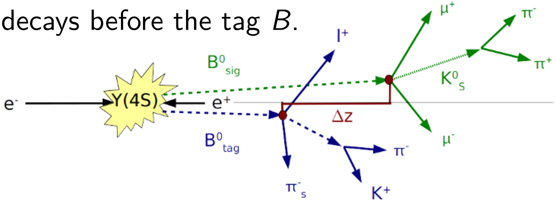

Flight distance and beam energies

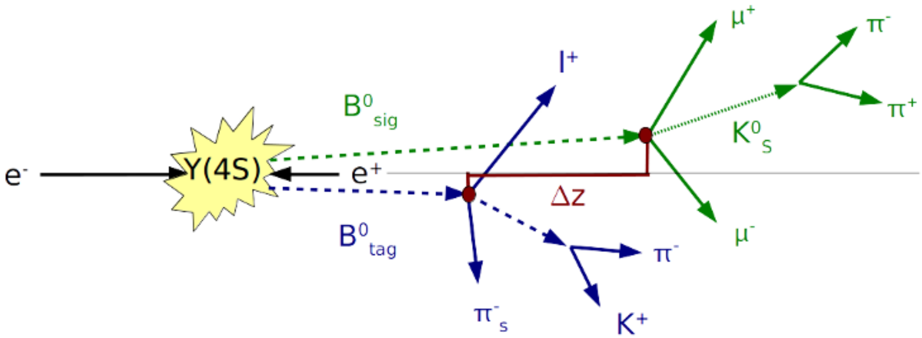

Flight distance and beam energies

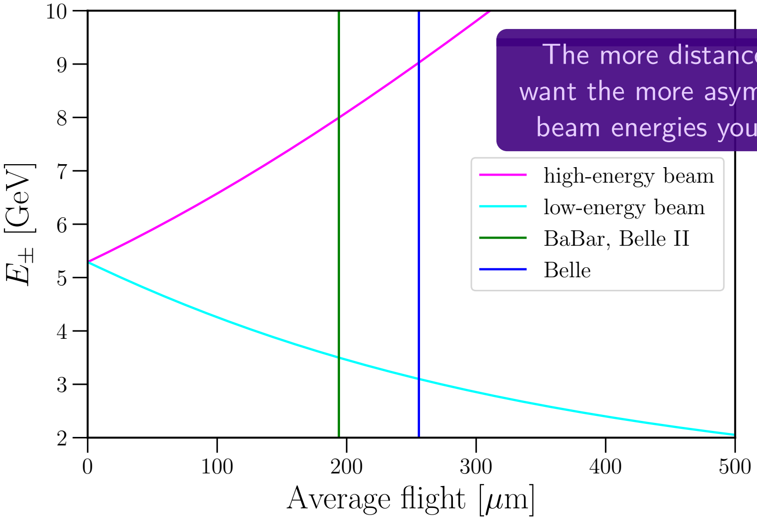

The more distance you want the more asymmetric beam energies you need

Beam-constrained observables

For B mesons the production process is $e^+e^- \to \Upsilon(4S) \to \bar{B}B$ followed by $B \to XYZ$

The reconstructed mass of the XYZ system must be equal to m_B and the energy in the rest frame to $E^*_{\text{beam}} = \frac{1}{2}\sqrt{s}$.

The second constraint is used by defining

$$\Delta E = E^*_B - E^*_{\text{beam}} = \frac{2p^{\mu}_B p^{\text{boost}}_{\mu} - s}{2\sqrt{s}}$$

with p_μ the four-momenta of the B and e^+e^- systems.

The B mass is also more precisely determined by replacing the measured B energy by the known beam energy

$$M_{\text{bc}} = \sqrt{E^*_{\text{beam}} - p^2_B}.$$

(m_{ES} in BaBar). A well-reconstructed B should have $(M_{\text{bc}}, \Delta E) = (M_B, 0)$

$B \to \ell^+\ell^-$ search at Belle

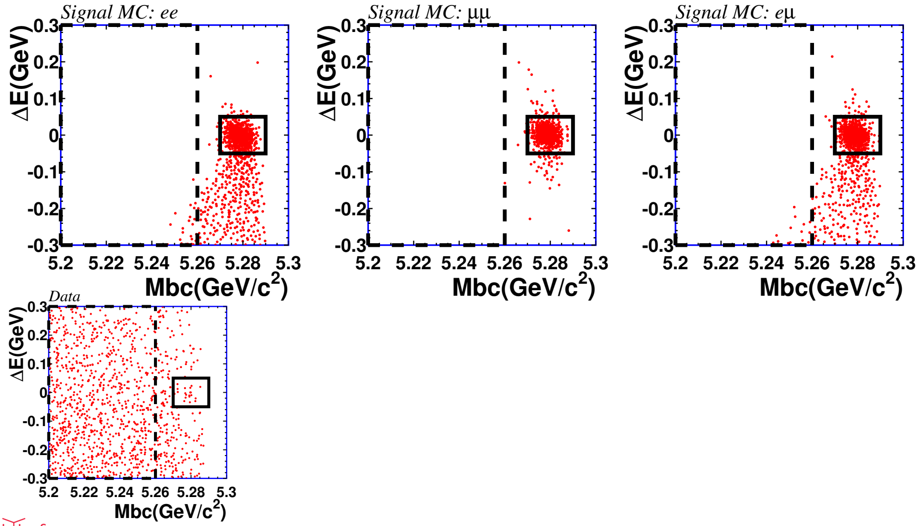

$B \to \ell^+\ell^-$ search at Belle

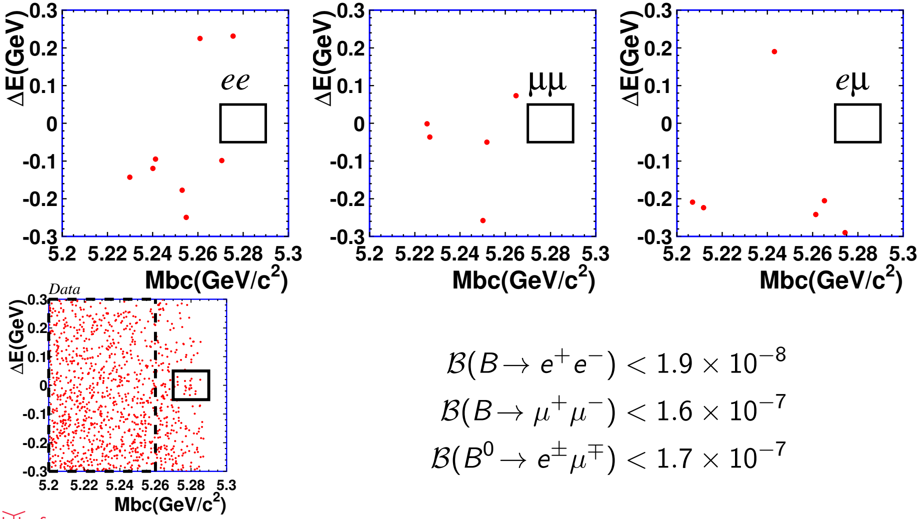

$$\mathcal{B}(B \to e^+e^-) < 1.9 \times 10^{-8}$$
$$\mathcal{B}(B \to \mu^+\mu^-) < 1.6 \times 10^{-7}$$
$$\mathcal{B}(B^0 \to e^\pm\mu^\mp) < 1.7 \times 10^{-7}$$

$B \to K^* \ell^+ \ell^-$ branching fractions

With $189\,\text{fb}^{-1}$ (2019–21, 197×10^6 BB pairs) see 22 $B \to K^* \mu^+ \mu^-$ and 18 $B \to K^* e^+ e^-$ using $K^+\pi^-$, $K^0_S\pi^0$ and $K^+\pi^0$.

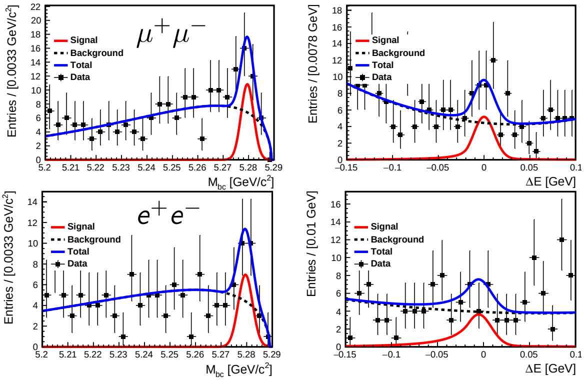

$$\mathcal{B}(B \to K^* \mu^+ \mu^-) = (1.19 \pm 0.31\,^{+0.08}_{-0.07}) \times 10^{-6}$$

$$\mathcal{B}(B \to K^* e^+ e^-) = (1.42 \pm 0.48 \pm 0.09) \times 10^{-6}$$

$$\mathcal{B}(B \to K^* \ell^+ \ell^-) = (1.25 \pm 0.30\,^{+0.08}_{-0.07}) \times 10^{-6}$$

Belle and LHCb

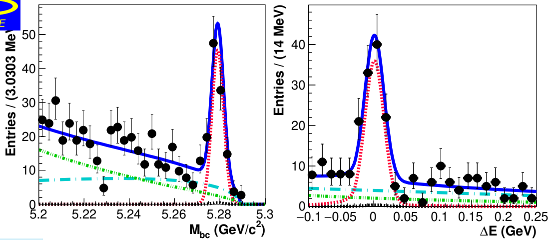

✔ Two handles: mass and B energy in $\Upsilon(4S)$ frame (ΔE)

[Belle, JHEP 03 (2021) 105]

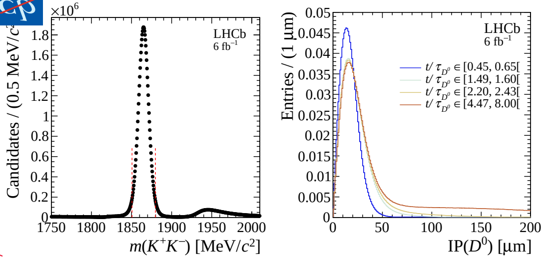

✔ Two handles: mass and pointing to PV

[PRD 104 (2021) 072010]

Belle versus LHCb: $B^+ \to K^+\mu^+\mu^-$

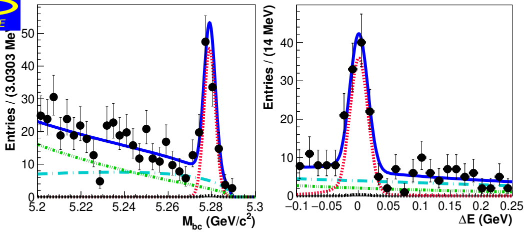

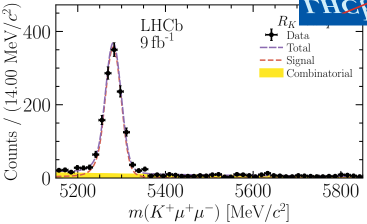

✔ Two handles: B mass and B energy in $\Upsilon(4S)$ frame (ΔE)

137 signal decays with 711 fb^{-1}

✔ Two handles: B mass and pointing to PV

1900 signal decays with 4 fb^{-1} at 13 TeV

Muons conversion factor: 2.5 ab^{-1} ↔ 1 fb^{-1}

Belle versus LHCb: $B^+ \to K^+ e^+ e^-$

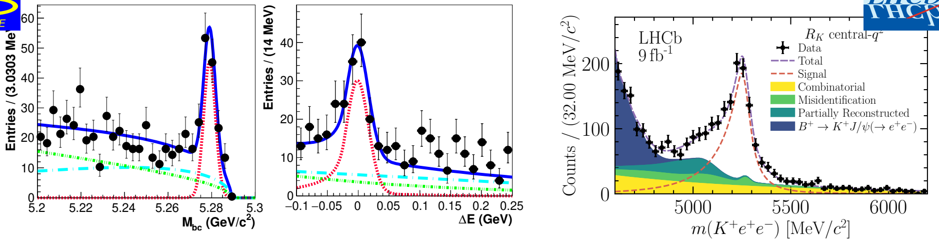

✔ Electron channels are as "easy" as muonic

138 signal decays with $711\,\text{fb}^{-1}$

✗ Bremsstrahlung makes electrons much more difficult

800 signal decays with $4\,\text{fb}^{-1}$ at 13 TeV

Electrons conversion factor: $1\,\text{ab}^{-1} \leftrightarrow 1\,\text{fb}^{-1}$

BESIII

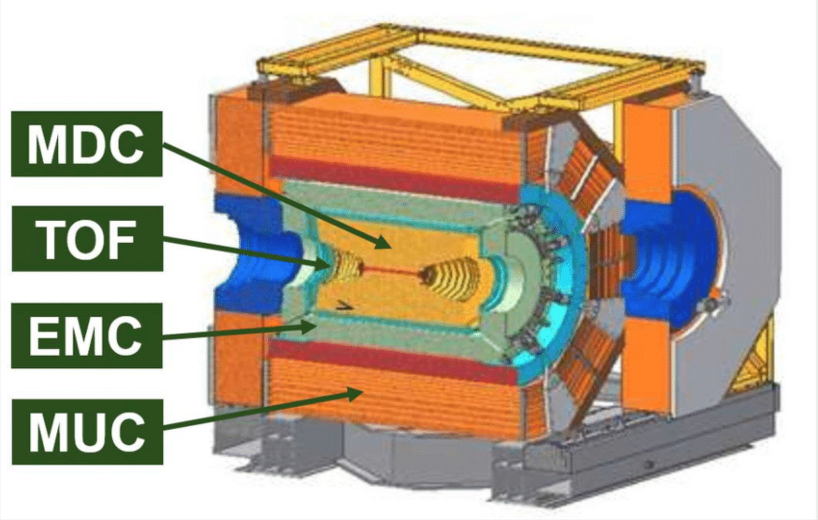

Conclusion

- Analyses exploit strengths of experiments
- Experiment designs are driven by physics
- There are multiple choices which leads to complementary experiments

[@pkoppenburg@sciencemastodon.com] [@pkoppenburg] [patrick.koppenburg@nikhef.nl]


THE
OTHER SIDE
Why do you need a reason?
© 1991 FarWorks, Inc. All rights reserved.

Backup

[Dedes, Dreiner, Nierste, PRL 87 (2001) 251804, arXiv:hep-ph/0108037]

$B_s^0 \to \mu^+\mu^-$ IN MINIMAL SUPERGRAVITY

$\mathcal{B}\,(B_s^0 \to \mu^+\mu^-)$ versus $\tan\beta$ and a_μ (of $g-2$)

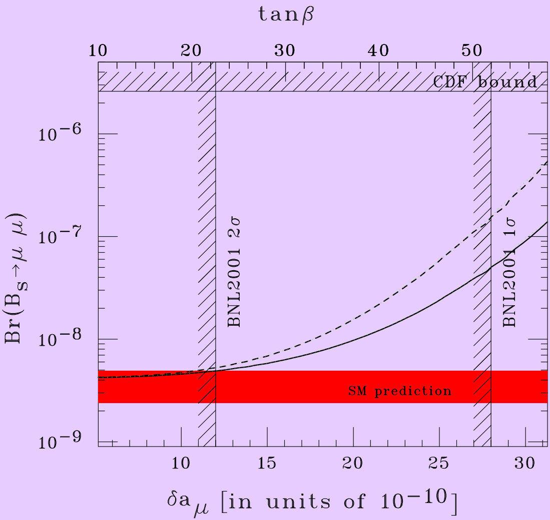

LEGACY MEASUREMENT OF $B_s^0 \to \mu^+\mu^-$

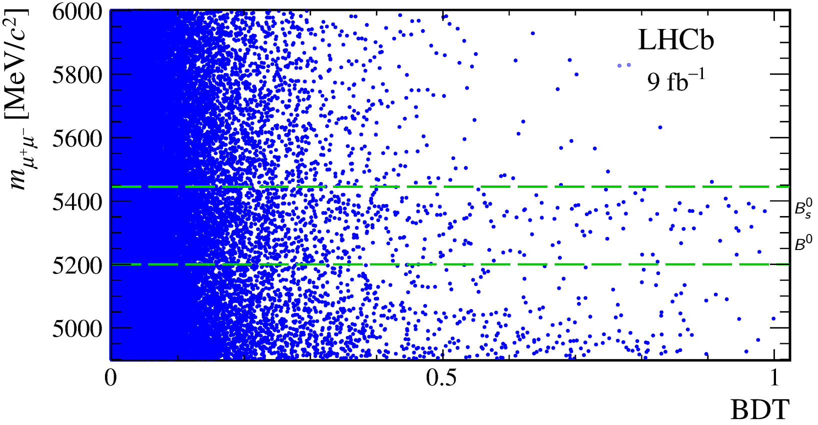

$B \to \mu^+\mu^-$ search using 2011–2018 data ($9\,\text{fb}^{-1}$) is done with a mass fit in bins of BDT output.

[B]

Legacy measurement of $B_s^0 \to \mu^+\mu^-$

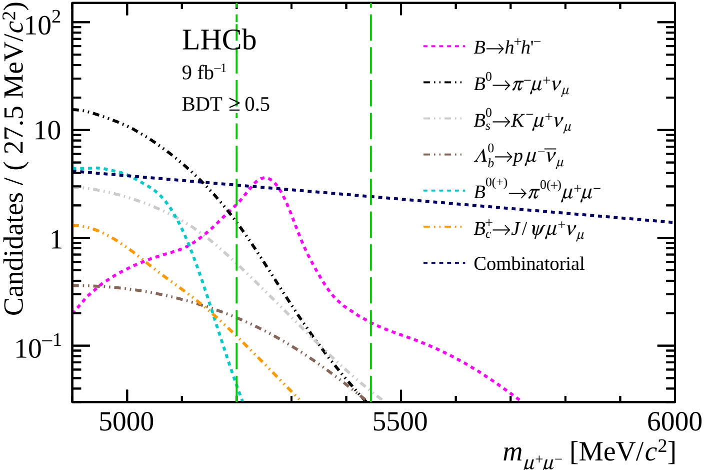

The BDT is optimised to fight combinatorial and specific backgrounds.

Legacy measurement of $B_s^0 \to \mu^+\mu^-$

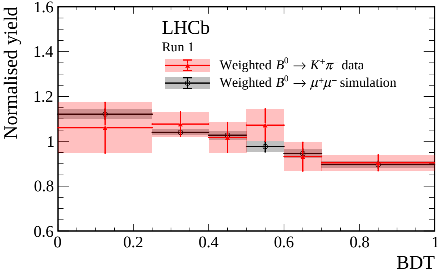

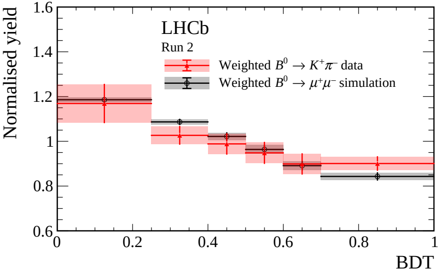

The BDT is calibrated using $B^0 \to K^+\pi^-$ decays, which have the same topology and are more abundant.

[B]

Legacy measurement of $B_s^0 \to \mu^+\mu^-$

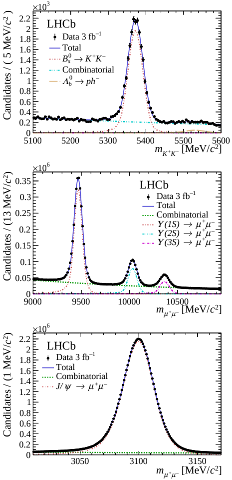

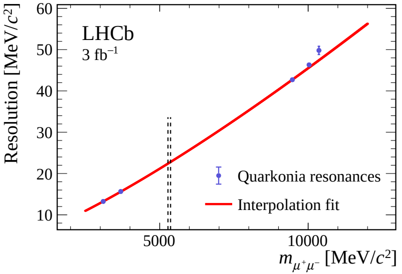

The mass resolution is calibrated using the decays $J/\psi \to \mu^+\mu^-$, $\psi(2S) \to \mu^+\mu^-$ and $\Upsilon([1,2,3]S) \to \mu^+\mu^-$ and interpolated to 23 MeV/c^2 at the B_s^0 mass. Checked with $B^0 \to K^+\pi^-$ and $B_s^0 \to K^+K^-$.

Here for Run 1

[B]

Legacy measurement of $B_s^0 \to \mu^+\mu^-$

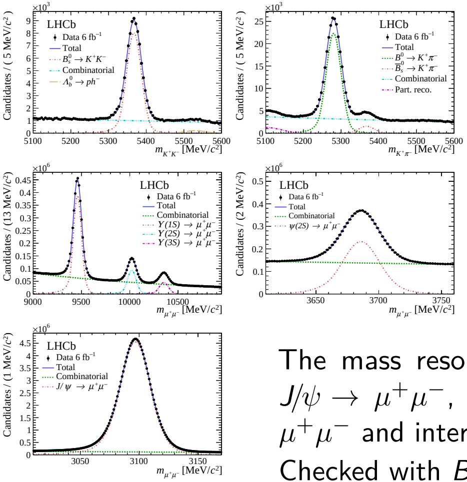

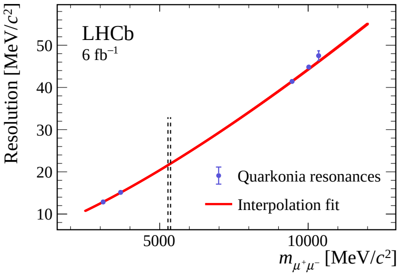

The mass resolution is calibrated using the decays $J/\psi \to \mu^+\mu^-$, $\psi(2S) \to \mu^+\mu^-$ and $\Upsilon([1,2,3]S) \to \mu^+\mu^-$ and interpolated to 23 MeV/c^2 at the B_s^0 mass. Checked with $B^0 \to K^+\pi^-$ and $B_s^0 \to K^+K^-$.

Here for Run 2

[B]

Legacy measurement of $B_s^0 \to \mu^+\mu^-$

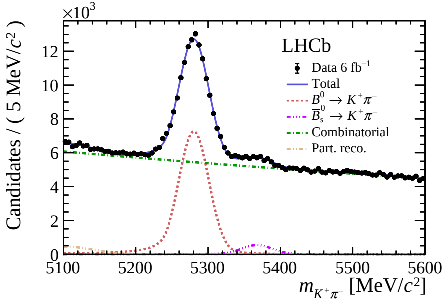

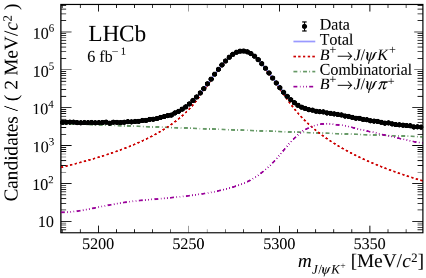

$B^0 \to K^+\pi^-$ and $B^+ \to J/\psi K^+$ are used to normalise the $B \to \mu^+\mu^-$ branching fractions. The factors are $a^{\text{norm}}_{B_s^0\to\mu^+\mu^-} = (2.49 \pm 0.09) \times 10^{-11}$ and $a^{\text{norm}}_{B^0\to\mu^+\mu^-} = (6.52 \pm 0.11) \times 10^{-12}$.

[B]

➜ Expecting 148±8 $B_s^0 \to \mu^+\mu^-$, 16±1 $B \to \mu^+\mu^-$ and about 3 $B_s^0 \to \mu^+\mu^-\gamma$

[LHCb, PRL 128 (2022) 041801, arXiv:2108.09284]

Legacy measurement of $B_s^0 \to \mu^+\mu^-$

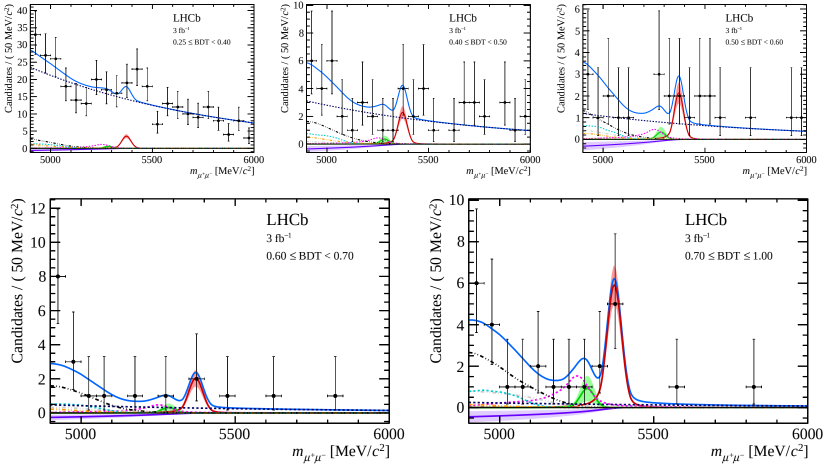

[B]

Mass fits are performed in bins of BDT output, for Run 1.

Legacy measurement of $B_s^0 \to \mu^+\mu^-$

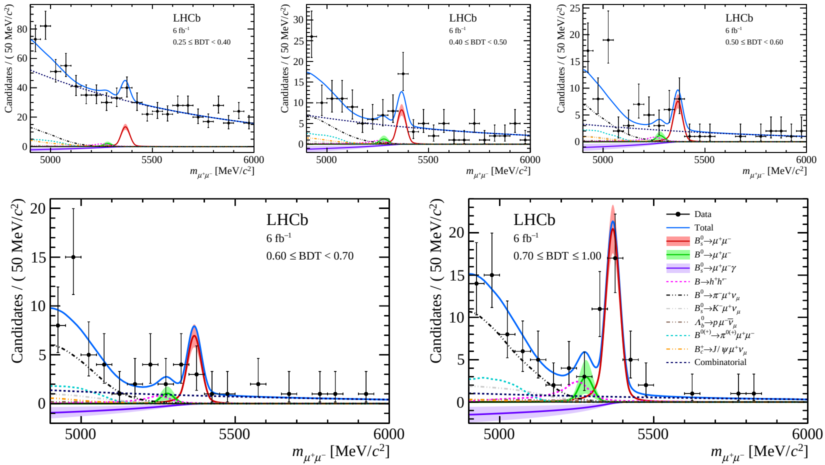

[B]

Mass fits are performed in bins of BDT output, for Run 2.

Legacy measurement of $B_s^0 \to \mu^+\mu^-$

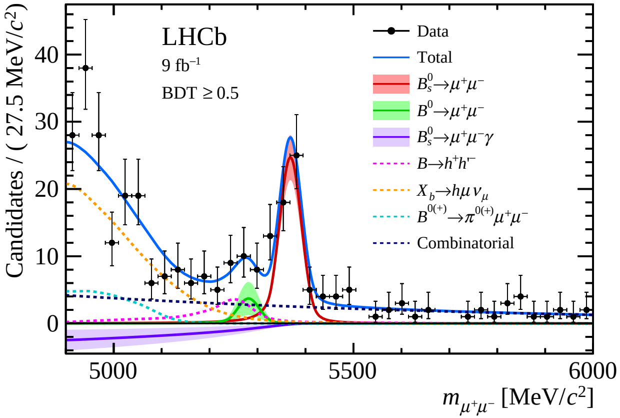

[B]

Mass plot shows candidates with BDT> 0.5.

The significances are 10σ for $B_s^0 \to \mu^+\mu^-$ and 1.7σ for $B^0 \to \mu^+\mu^-$.

Legacy measurement of $B_s^0 \to \mu^+\mu^-$

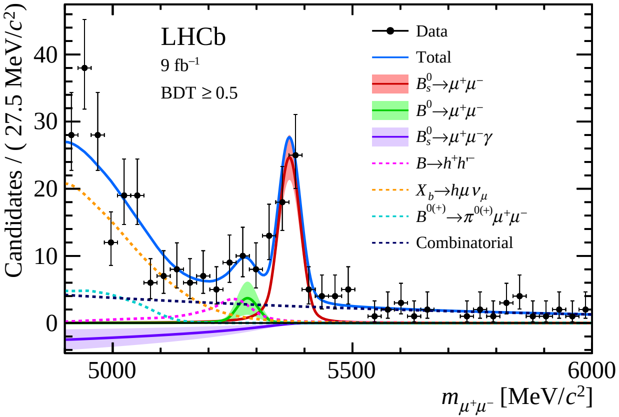

The results $\mathcal{B}(B_s^0 \to \mu^+\mu^-) = (3.09\,^{+0.46}_{-0.43}\,^{+0.15}_{-0.11}) \times 10^{-9}$ and $\mathcal{B}(B^0 \to \mu^+\mu^-) = (1.2\,^{+0.8}_{-0.7} \pm 0.1) \times 10^{-10}$ are consistent with the SM.

[B]

Legacy measurement of $B_s^0 \to \mu^+\mu^-$

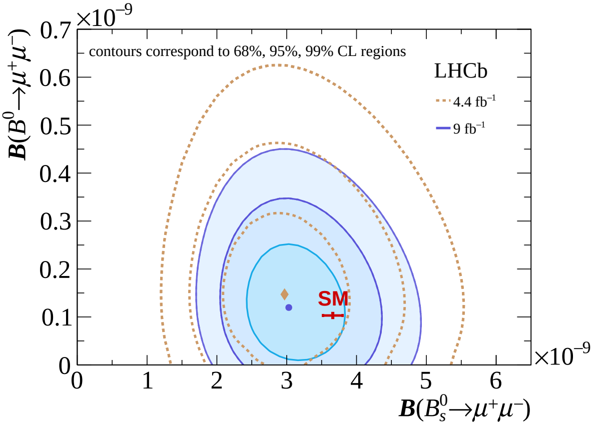

[Beneke, Bobeth, Szafron, JHEP 10 (2019) 232]

The results $\mathcal{B}(B_s^0 \to \mu^+\mu^-) = (3.09\,^{+0.46}_{-0.43}\,^{+0.15}_{-0.11}) \times 10^{-9}$ and $\mathcal{B}(B^0 \to \mu^+\mu^-) = (1.2\,^{+0.8}_{-0.7} \pm 0.1) \times 10^{-10}$ are consistent with the SM.

Legacy measurement of $B_s^0 \to \mu^+\mu^-$

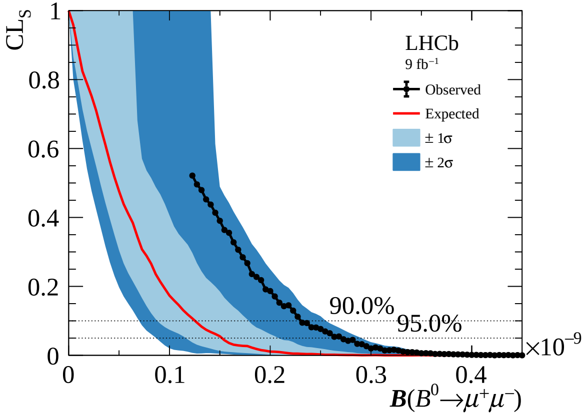

As no excess of $B^0 \to \mu^+\mu^-$ is found, a limit at 2.6×10^{-10} at 95% confidence level is set.

[B]

Legacy measurement of $B_s^0 \to \mu^+\mu^-$

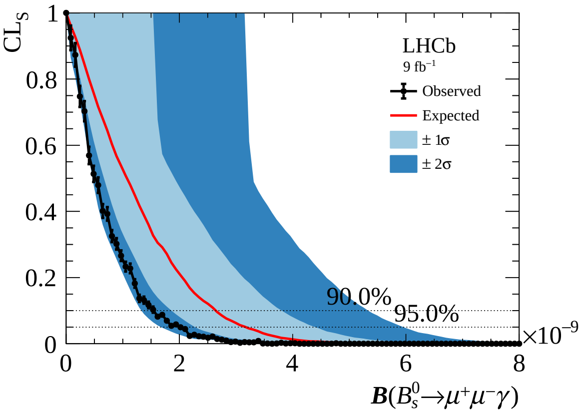

$\mathcal{B}(B_s^0 \to \mu^+\mu^-\gamma)_{m(\mu^+\mu^-)>4.9\,\text{GeV}} = (-2.5 \pm 1.4 \pm 0.8) \times 10^{-9}$. As no excess is found, a limit at 2.0×10^{-9} at 95% confidence level is set.

[B]

Legacy measurement of $B^0_s \to \mu^+\mu^-$

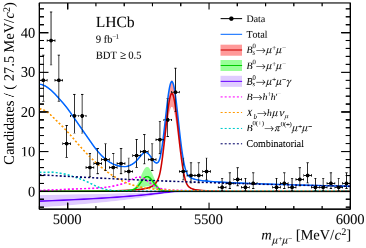

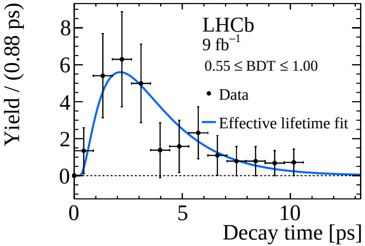

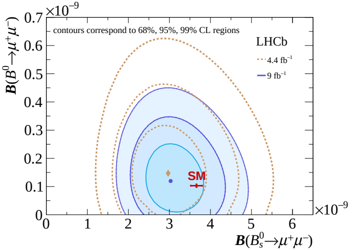

With 2011–2018 LHCb data ($9\,\text{fb}^{-1}$):

$$\mathcal{B}(B^0_s \to \mu^+\mu^-) = (3.09\,^{+\,0.46}_{-\,0.43}\,^{+\,0.15}_{-\,0.11}) \times 10^{-9}$$

$$\mathcal{B}(B^0 \to \mu^+\mu^-) = (1.2\,^{+\,0.8}_{-\,0.7} \pm 0.1) \times 10^{-10}$$

Effective lifetime:

$$\tau^{\text{eff}}_{B^0_s\to\mu^+\mu^-} = 2.07 \pm 0.29 \pm 0.03\ \text{ps}$$

[B]

LHCb Trigger in Run 2

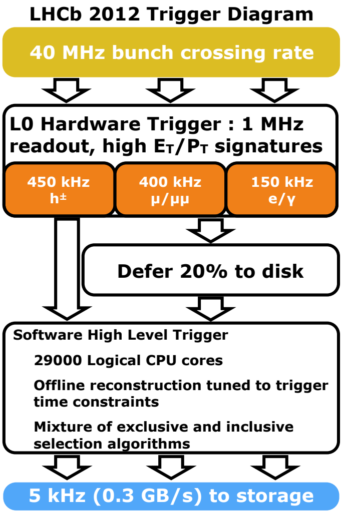

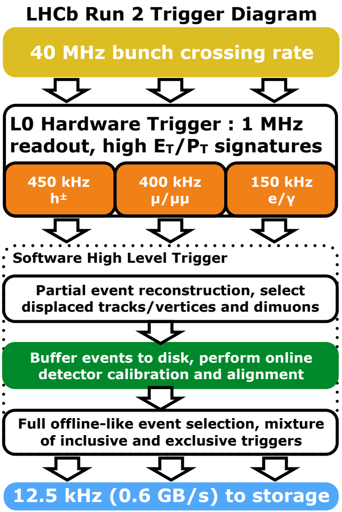

LHCb Trigger in Run 2

Events are buffered on disk (10 PB) while calibrations are being run.

→ Offline-quality trigger objects available for analysis.

- Disk → more CPU. The full reconstruction can also be run during LHC downtime.

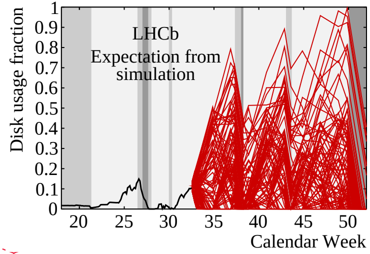

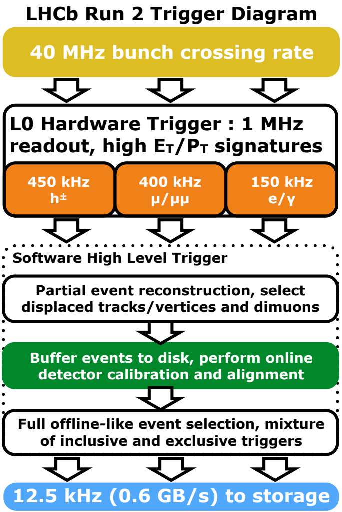

LHCb Trigger in Run 2

Events are buffered on disk (10 PB) while calibrations are being run.

→ Offline-quality trigger objects available for analysis.

- Disk → more CPU. The full reconstruction can also be run during LHC downtime.

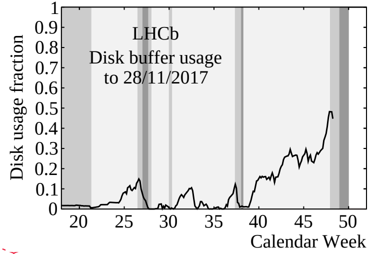

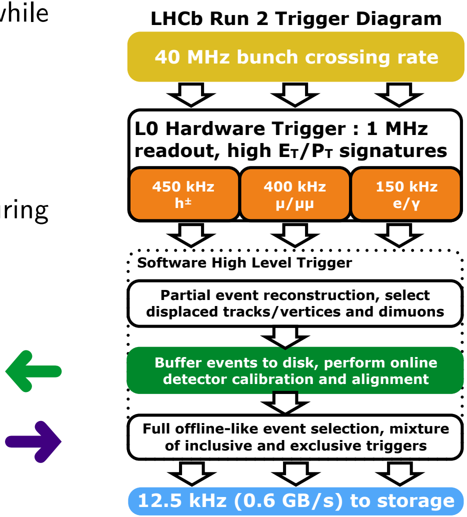

TURBO

We perform a full calibration in real time. The output is ready to be used for physics.

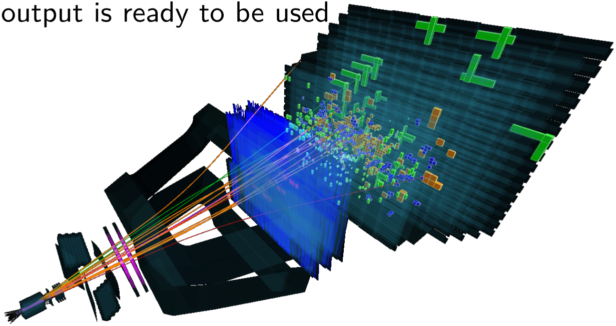

Plenty of collision events discarded, while the interesting are kept.

TURBO

We perform a full calibration in real time. The output is ready to be used for physics.

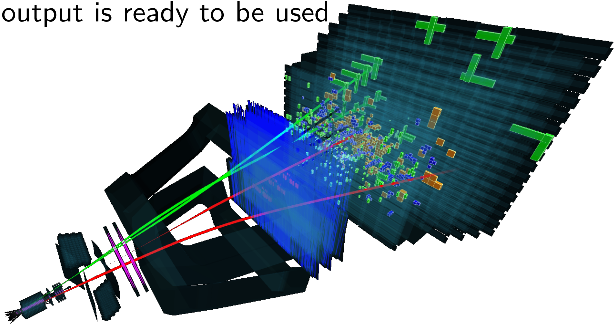

TURBO then stores only the information needed for the analysis

➜ Huge savings in time and cost

TURBO

We perform a full calibration in real time. The output is ready to be used for physics.

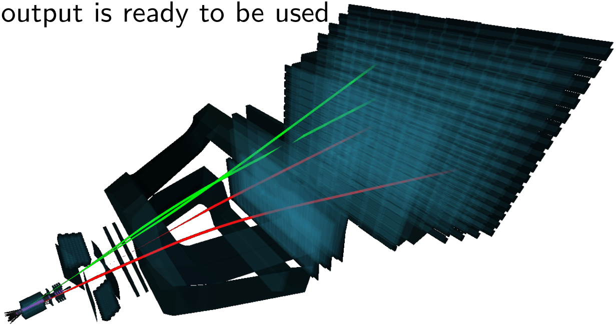

TURBO then stores only the information needed for the analysis

➜ Huge savings in time and cost

[JINST 3 (2008) S08005]

LHCb Detector (Run 1–2)

Forward detector: many b hadrons produced forward at LHC, $(144 \pm 1 \pm 21)$ µb in acceptance at 13 TeV [PRL 118 (2017) 052002]

- Warm dipole magnet. Polarity can be reversed
- ✔ Good momentum and position resolution [JINST 10 (2015) P02007]
  - Vertex detector gets 8mm to the beam

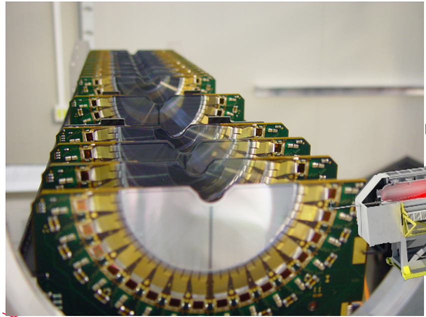

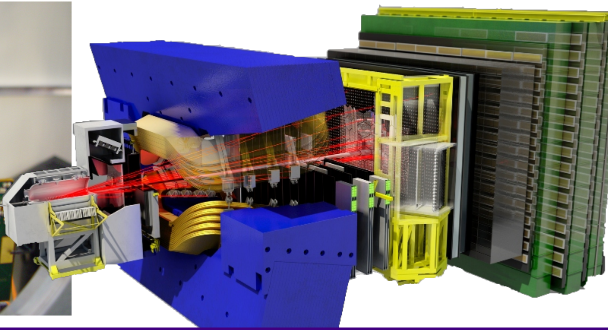

LHCb Detector (Run 1–2)

Forward detector: many b hadrons produced forward at LHC, $(144 \pm 1 \pm 21)\,\mu$b in acceptance at 13 TeV [PRL 118 (2017) 052002]

- Warm dipole magnet. Polarity can be reversed
- ✔ Good momentum and position resolution [JINST 10 (2015) P02007]
- ✔ Excellent Particle ID [EPJC 73 (2013) 2431]

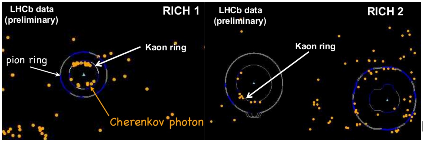

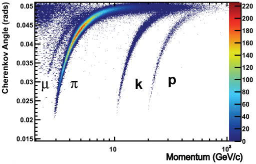

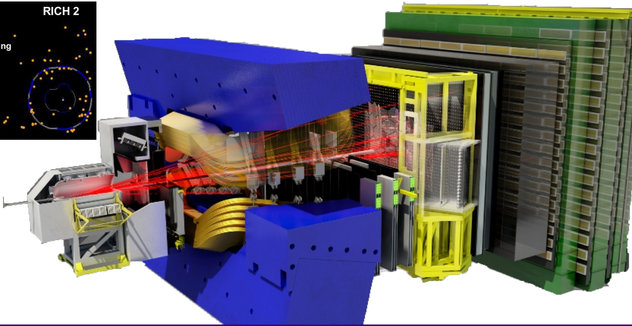


Rien ne doit déranger
un honnête homme qui boit
www.koppenburg.org


www.koppenburg.org


www.koppenburg.org


www.koppenburg.org


www.koppenburg.org


www.koppenburg.org


www.koppenburg.org


www.koppenburg.org


www.koppenburg.org

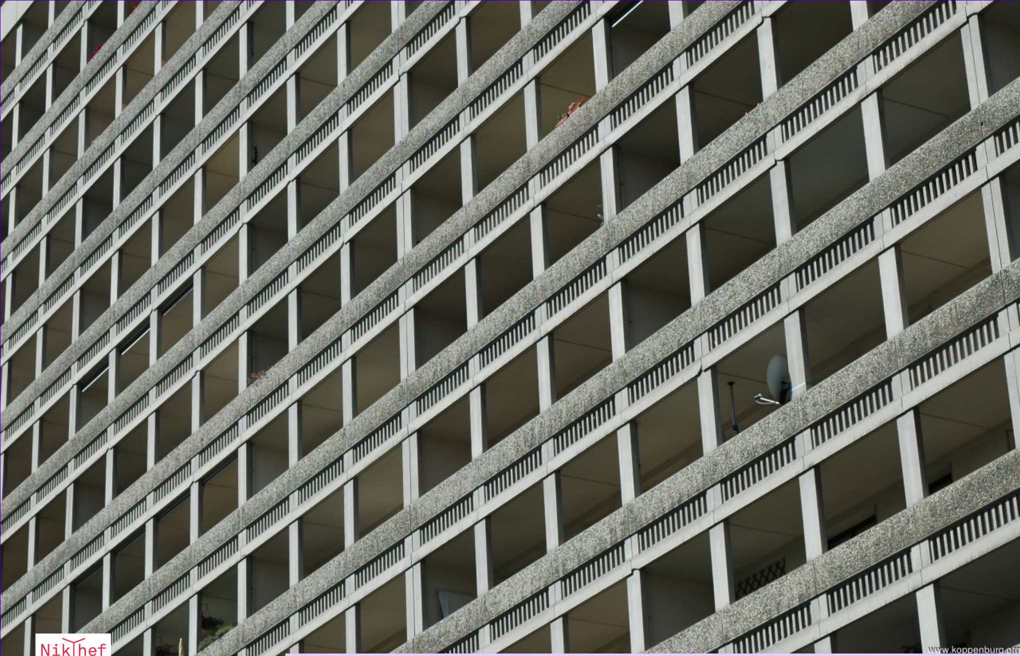
www.koppenburg.org


www.koppenburg.org

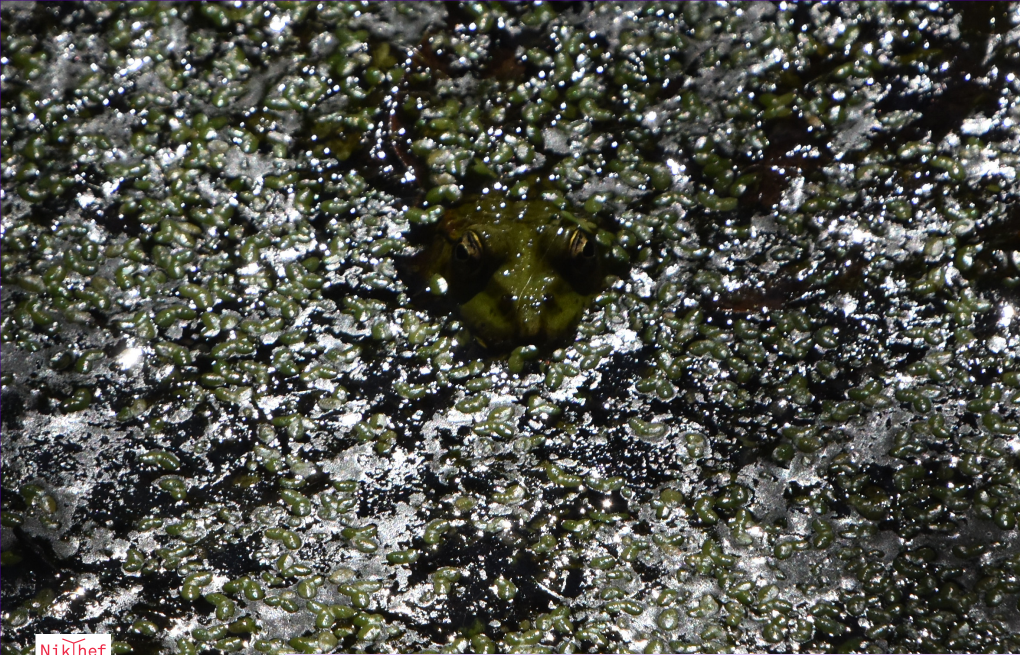


04/09/2019 - patrick@koppenburg.ch


04/09/2019 - patrick@koppenburg.ch


04/09/2019 - patrick@koppenburg.ch


04/09/2019 - patrick@koppenburg.ch


04/09/2019 - patrick@koppenburg.ch


04/09/2019 - patrick@koppenburg.ch


04/09/2019 - patrick@koppenburg.ch


(g) 05/09/2019 - patrick@koppenburg.ch